



Available online at <http://scik.org>

Commun. Math. Biol. Neurosci. 2025, 2025:146

<https://doi.org/10.28919/cmbn/9641>

ISSN: 2052-2541

## AUGMENTATION IN COMPETITION INTERACTION MODEL: A DISCRETE TIME OPTIMAL CONTROL ANALYSIS

MUNKAILA DASUMANI<sup>1,\*</sup>, SUZANNE LENHART<sup>2</sup>, GLADYS K. ONYAMBU<sup>3</sup>, STEPHEN E. MOORE<sup>4</sup>

<sup>1</sup>Department of Mathematics, Institute for Basic Sciences, Technology and Innovation, Pan African University,  
Nairobi, Kenya

<sup>2</sup>Department of Mathematics, University of Tennessee, Knoxville, Tennessee, USA

<sup>3</sup>Department of Zoology, Jomo Kenyatta University of Agriculture and Technology, Nairobi, Kenya

<sup>4</sup>Department of Mathematics, University of Cape Coast, Cape Coast, Ghana

Copyright © 2025 the author(s). This is an open access article distributed under the Creative Commons Attribution License, which permits unrestricted use, distribution, and reproduction in any medium, provided the original work is properly cited.

**Abstract.** Many species are classified as threatened or endangered and are declining due to factors such as competition for limited resources. Competition affects the fitness of both populations as one organism's use of a scarce resource decreases its availability to the other. In this study, a discrete-time competition interaction model with controls is formulated. We consider four populations represented by a discrete competition model with strong Allee effects. We define two objective functionals that account for linear and nonlinear representations of the translocation costs of the reserve populations at each time step. The objective functionals seek to maximize the populations and minimize the cost of augmentation. We employ the generalization of Pontryagin's Maximum Principle for the optimal control of discrete-time state systems to obtain the necessary conditions. The discrete version of the forward-backward sweep method is employed to solve the optimality system numerically. The short-term and long-term qualitative dynamics of the model are discussed through the numerical simulations. Objective functional values indicating a percentage increase with optimal controls are calculated for each plot. The numerical simulation examines various scenarios, including the effects of cost constants, competition coefficients, and augmentation coefficients in the model.

---

\*Corresponding author

E-mail address: [munkaila5@gmail.com](mailto:munkaila5@gmail.com)

Received October 14, 2025

**Keywords:** discrete-time difference equations; forward-backward sweep method; strong Allee effects; competition interaction model; species augmentation.

**2020 AMS Subject Classification:** 92D25.

## 1. BACKGROUND

Phenomena such as outbreaks of diseases, competition, predation, and urbanization have been significant indicators of the decline or extinction of several endangered species. A substantial number of species are classified as threatened or endangered, with about 77% experiencing population declines due to anthropogenic variables like habitat destruction [1, 2], decreased prey populations [3], competition for limited resources, human poaching and persecution [4, 5, 6, 7, 8]. There are multiple extinct birds and animals, and several more are in danger of going extinct. For example, the Dolphin in China, Spix's macaw in Brazil, the Zanzibar leopard in Tanzania, the Pinta Island Tortoise (The Galápagos), and the Baiji River are thought to be extinct. Several other extinct animals and the potential causes of their extinction are reported in [9].

Despite the multiple attempts to protect individual organisms and habitats, several species have been identified as being vulnerable or threatened, and most are on the edge of extinction [5, 4]. To prevent the worldwide loss of biodiversity due to species extinction, species augmentations are increasingly being used as a conservation technique to safeguard threatened species from going extinct [10, 11, 12, 13]. Species augmentation, which includes supplementing declining species populations with captive-bred individuals or using captive-bred individuals to restore an extinct species population [14, 15], has recently gained weight in conservation policy.

Over the last few decades, translocation of species for augmentation, or transfers of animals to avoid population extinctions, has increased considerably [16]. A study conducted by Romain-Bondi et al. [17] on a targeted bear species population indicated that its survival was extremely unusual and recommended an augmentation technique. The successful reintroduction of African wild dogs (*Lycaon pictus*) to Gorongosa National Park in Mozambique has been carried out by Bouley et al. [18]. Their study describes the first transboundary translocation and

reintroduction of founding packs of wild dogs to Gorongosa over a 28-month study period. The research conducted by Funabashi [19] on the augmentation of plants in synecoculture offered a theoretical foundation and novel discoveries that create a special framework for protecting our natural environment. An investigation carried out on the huemul deer species population offered augmentation approaches to boost the huemul's population, which had severely decreased to only one individual [20]. Hearne and Swart [21] explored the species translocation technique for conserving Rhino population from high-density to low-density habitats.

In addition to the above augmentation efforts, the study of critically endangered succulent plant species *Euphorbia clivicola* with four management options suggested augmentation as the management strategy [22]. Hedrick [23] developed a model to predict the chances for the recovery of a Florida panther population using an augmentation technique. A rescue of an endangered carnivore using an augmentation strategy was investigated by Manlick et al. [24]. In addition, the optimal genetic augmentation strategies for a threatened species using a continent-island model have been studied by Bodine and Martinez [25]. Augmentation in a competition interaction population model of differential equations was investigated in [8], where individuals were to be translocated from the reserve regions to the target/endangered regions.

While the logistic growth model may be useful in some situations, there are times when a species' future survival is determined by its initial growth threshold, a phenomenon called the Allee effect [26, 27]. The biological phenomenon, Allee effect, was first described by Allee in the 1930s [28, 27, 29]. This explains a direct association between the size of a species population and the rate of growth of each individual within the group [30]. The Allee effects can occur by different circumstances happening in very small populations, such as difficulty in finding mates [31], competition for limited resources, reduction in foraging effectiveness, and diminished defenses against predators [29, 31, 32]. It can be weak or strong. The population exhibiting a strong Allee effect has a critical population threshold below which the growth rate is declining, and above which the population grows positively [32, 33, 34]. Endangered/target populations requiring augmentation are often populations small in density and exhibiting a decline in population size. We assume in this work that the populations grow based on a strong

Allee effect; hence, the endangered or target populations are currently below some critical density and are declining.

Discrete-time difference equations have been employed to model a variety of population dynamics using optimal control theory. The ability to depict real-world scenarios and provide effective results for numerical simulations has been one of the many reasons discrete-time models have received significant contributions in recent years. An optimal control of harvest timing in discrete population models is studied in [35]. El Bhih et al. [36] have examined a spatiotemporal prey-predator discrete model and optimal controls for environmental sustainability in the multifishing areas of Morocco. Optimal control theory applied to managing an invasive plant species using discrete-time difference equations is provided by Whittle et al. [37]. In addition, Bodine et al. [11] examined the comparison of discrete models for optimal control of species augmentation with different possible orders of events.

Optimal control theory applied to a discrete model of species augmentation with a competition relationship has not been explored. In this current work, we investigate augmentation in a competition population model using discrete difference equations. We will consider two objective functionals that account for the cost of translocating individuals from the reserve region to the target zone. The generalization of the discrete version of the forward-backward sweep method will be used to solve the optimality systems. Again, short-term and long-term qualitative dynamics of the model will be discussed through the numerical simulations. The rest of the article is arranged as follows: Formulation of the discrete-time competition model with controls is carried out in Section 2, objective functionals and optimality systems are discussed in Section 3, simulations results and explanations are presented in Section 4, and the conclusion of the work is summarised in Section 5.

## 2. DISCRETE-TIME COMPETITION MODEL WITH CONTROLS

Competition decreases the fitness of both species since one species' usage of the scarce resource decreases its availability to the other [38, 10]. The competitive exclusive principle states that if two species compete for the same limited resources, one will go extinct. Some mathematical models describing the competitive exclusive principle are competition between protozoan

species [39]; stable coexistence of two competitors [40, 41, 42, 43]; structured competitive interaction population [44]; and discrete competitive and cooperative models of Lotka–Volterra type [45]. A species can become endangered or extinct if it loses its food and habitat. One way to reduce the loss of species is by adopting an augmentation strategy, where individuals can be translocated from reserve populations to augment the declining species at a minimum cost [10]. In this work, we describe a competition model that exhibits a very general principle that is realized to hold in nature, thus, when two different species engage in competition over a limited resource, one of the species often becomes extinct [38].

In formulating the discrete model, we will consider four populations: two of them are considered to be competing for the same limited resources, and the remaining two are reserved in their habitats. Initially, all four populations are considered to be exhibiting strong Allee effect; see, for example, [46, 47]. Grey squirrels and red squirrels, lions and hyenas, Sunfish and bass found in freshwater are some examples of interacting species that represent our model.

The following nonlinear discrete-time difference equations describe the dynamics of two competing interaction populations  $X$  and  $Y$  of the discrete version of the Lotka–Volterra competition model, see the books by Murray (2002) and Kot (2001) [38, 46]

$$(1) \quad \begin{aligned} X_{t+1} - X_t &= r_1 X_t \left( 1 - \frac{X_t}{K_X} \right) - r_1 m_1 \frac{X_t Y_t}{K_X}, \\ Y_{t+1} - Y_t &= r_2 Y_t \left( 1 - \frac{Y_t}{K_Y} \right) - r_2 m_2 \frac{X_t Y_t}{K_Y}, \end{aligned}$$

where  $X_t$  and  $Y_t$  are the population sizes of the two competing species,  $r_1$  and  $r_2$  are the growth rates of the populations  $X_t$  and  $Y_t$  at time  $t$ , respectively. The parameters  $m_1$  measures the competitive effect of population  $Y_t$  on  $X_t$  and  $m_2$  measures the competitive effect of population  $X_t$  on  $Y_t$ . Also,  $K_X$  and  $K_Y$  are the environmental carrying capacities of the populations  $X_t$  and  $Y_t$ , respectively.

The species  $X$  and  $Y$  are declining due to small population sizes, which can be a result of competition for limited resources, and hence they are referred to as endangered/targeted species [8, 10, 11]. Therefore, there is a critical threshold below which the population declines towards extinction due to small population sizes caused by competition for limited resources. Thus, we assume the populations are subjected to strong Allee effects. By considering Allee effects in

the populations, system (1) becomes

$$(2) \quad \begin{aligned} X_{t+1} - X_t &= r_1 X_t \left(1 - \frac{X_t}{K_X}\right) \left(\frac{X_t}{K_X} - a\right) - r_1 m_1 \frac{X_t Y_t}{K_X}, \\ Y_{t+1} - Y_t &= r_2 Y_t \left(1 - \frac{Y_t}{K_Y}\right) \left(\frac{Y_t}{K_Y} - b\right) - r_2 m_2 \frac{X_t Y_t}{K_Y}, \end{aligned}$$

where  $a$  and  $b$  are the strong Allee effect constants where  $a, b \in (0, 1)$ . Again,  $aK_X$  and  $bK_Y$  are Allee thresholds such that for  $X_t < aK_X$  the population size of  $X_t$  is declining and for  $Y_t < bK_Y$  the population size of  $Y_t$  is declining.

Again, two additional reserve species,  $R_X$  and  $R_Y$ , are kept separately in their habitats and are viable sources for harvesting and translocating individuals to augment the endangered species  $X$  and  $Y$ , respectively. The reserve species satisfy the discrete-time difference equations

$$(3) \quad \begin{aligned} (R_X)_{t+1} - (R_X)_t &= r_3 (R_X)_t \left(1 - \frac{(R_X)_t}{K_{R_X}}\right) \left(\frac{(R_X)_t}{K_{R_X}} - c\right), \\ (R_Y)_{t+1} - (R_Y)_t &= r_4 (R_Y)_t \left(1 - \frac{(R_Y)_t}{K_{R_Y}}\right) \left(\frac{(R_Y)_t}{K_{R_Y}} - d\right), \end{aligned}$$

where  $(R_X)_t$  and  $(R_Y)_t$  are population densities or sizes,  $r_3$  and  $r_4$  are the growth rates of the reserve populations  $(R_X)_t$  and  $(R_Y)_t$ , respectively at time  $t$ ,  $K_{R_X}$  and  $K_{R_Y}$  are the carrying capacities, and  $cK_{R_X}$  and  $dK_{R_Y}$  denote the Allee thresholds such that  $c, d \in (0, 1)$ .

Furthermore, there is a vector of controls  $u_1 = (u_{1,0}, u_{1,1}, \dots, u_{1,T-1})$  and  $u_2 = (u_{2,0}, u_{2,0}, \dots, u_{2,T-1})$ , where  $u_{1,t}$  and  $u_{2,t}$  are the portions of the reserve populations that are harvested and translocated to the target populations at time step  $t$ . Now, combining Equations (2) and (3) together with controls  $u_{1,t}$  and  $u_{2,t}$ , our discrete-time species augmentation model for the competition species becomes

$$(4) \quad \begin{aligned} X_{t+1} - X_t &= r_1 X_t \left(1 - \frac{X_t}{K_X}\right) \left(\frac{X_t}{K_X} - a\right) - r_1 m_1 \frac{X_t Y_t}{K_X} + u_{1,t} (R_X)_t, \\ Y_{t+1} - Y_t &= r_2 Y_t \left(1 - \frac{Y_t}{K_Y}\right) \left(\frac{Y_t}{K_Y} - b\right) - r_2 m_2 \frac{X_t Y_t}{K_Y} + u_{2,t} (R_Y)_t, \\ (R_X)_{t+1} - (R_X)_t &= r_3 (R_X)_t \left(1 - \frac{(R_X)_t}{K_{R_X}}\right) \left(\frac{(R_X)_t}{K_{R_X}} - c\right) - u_{1,t} (R_X)_t, \\ (R_Y)_{t+1} - (R_Y)_t &= r_4 (R_Y)_t \left(1 - \frac{(R_Y)_t}{K_{R_Y}}\right) \left(\frac{(R_Y)_t}{K_{R_Y}} - d\right) - u_{2,t} (R_Y)_t, \end{aligned}$$

with the subscripts representing the time steps. Given the carrying capacities of the four populations

$$(5) \quad \begin{cases} x_{1,t} \equiv \frac{X_t}{K_X}, \\ y_{1,t} \equiv \frac{Y_t}{K_Y}, \\ x_{2,t} \equiv \frac{(R_X)_t}{K_{R_X}}, \\ y_{2,t} \equiv \frac{(R_Y)_t}{K_{R_Y}}, \end{cases}$$

and for  $t = 0, 1, \dots, T - 1$ , the rescaled version of the model system (4) is obtained as

$$(6) \quad \begin{aligned} x_{1,t+1} &= x_{1,t} + r_1 x_{1,t} (1 - x_{1,t}) (x_{1,t} - a) - \phi_1 x_{1,t} y_{1,t} + \rho_1 u_{1,t} x_{2,t}, \\ y_{1,t+1} &= y_{1,t} + r_2 y_{1,t} (1 - y_{1,t}) (y_{1,t} - b) - \phi_2 x_{1,t} y_{1,t} + \rho_2 u_{2,t} y_{2,t}, \\ x_{2,t+1} &= x_{2,t} + r_3 x_{2,t} (1 - x_{2,t}) (x_{2,t} - c) - u_{1,t} x_{2,t}, \\ y_{2,t+1} &= y_{2,t} + r_4 y_{2,t} (1 - y_{2,t}) (y_{2,t} - d) - u_{2,t} y_{2,t}, \end{aligned}$$

with the initial conditions  $x_{1,0} > 0, y_{1,0} > 0, x_{2,0} > 0, y_{2,0} > 0$ , where

$$(7) \quad \begin{cases} \phi_1 = \frac{r_1 m_1 K_Y}{K_X}, \\ \phi_2 = \frac{r_2 m_2 K_X}{K_Y}, \\ \rho_1 = \frac{K_{R_X}}{K_X}, \\ \rho_2 = \frac{K_{R_Y}}{K_Y}. \end{cases}$$

Moreover, the vectors

$$(8) \quad \begin{cases} x_1 = (x_{1,0}, x_{1,1}, \dots, x_{1,T}), \\ y_1 = (y_{1,0}, y_{1,1}, \dots, y_{1,T}), \\ x_2 = (x_{2,0}, x_{2,1}, \dots, x_{2,T}), \\ y_2 = (y_{2,0}, y_{2,1}, \dots, y_{2,T}), \end{cases}$$

represent the vector of the states, where  $x_{1,t}$ ,  $y_{1,t}$ ,  $x_{2,t}$  and  $y_{2,t}$  are the biomass densities of the rescaled populations. For discrete-time optimal control models, the state vectors often have an additional component than the control vectors.

### 3. OBJECTIVE FUNCTIONALS AND OPTIMALITY SYSTEMS

In the maximization of the objective functionals, the costs may increase quadratically or linearly, or a combination of the two. For this reason, we will consider two objective functionals in this current study. Because there is a cost associated with moving individuals from reserve areas to supplement the target areas at each time step, we shall investigate strategies to reduce cost. We will apply different weights to the endangered and the reserve populations to maximize the total population  $(x_{1,t} + y_{1,t} + x_{2,t} + y_{2,t})$  at each time step in both objective functionals. The target populations  $x_{1,t}$  and  $y_{1,t}$  are initially assumed to have population sizes  $x_{1,0}$  and  $y_{1,0}$  below their thresholds  $a$  and  $b$ , respectively. Also, the reserve populations  $x_{2,t}$  and  $y_{2,t}$  are have population sizes  $x_{2,0}$  and  $y_{2,0}$  above their thresholds  $c$  and  $d$ , respectively. Hence,  $x_{1,0} < a, y_{1,0} < b, x_{2,0} > c$  and  $y_{2,0} > d$ . The discrete-time optimal control of the augmentation model is formulated with objective functionals to be maximized based on assumptions above.

First, we will consider an objective functional that has the states at the final time step (with weights) before delving into an objective functional that has the states (with weights) over the time steps. Again, optimality systems representing the two objective functionals will be obtained.

#### 3.1. Objective Functional with Linear and Quadratic Cost Terms.

In this section, we construct an objective functional that accounts for linear and nonlinear costs increases as the proportion of the reserve population translocated at each time step increases. Therefore, the augmentation technique defined in this section aims to maximize the target interaction populations at each time step with both linear and quadratic cost functions of the controls and maximize the difference between the benefits (endangered population levels at each time step) and the costs. We apply different weights to the target and the reserve species populations to maximize the total population  $(x_{1,t} + y_{1,t} + x_{2,t} + y_{2,t})$  at each time step. The maximization objective functional with both linear and quadratic costs to be maximized is constructed

$$(9) \quad \mathbf{J}(u_1, u_2) = x_{1,T} + y_{1,T} + Cx_{2,T} + Dy_{2,T} - \sum_{t=0}^{T-1} A_1 u_{1,t}^2 + A_2 u_{1,t} + B_1 u_{2,t}^2 + B_2 u_{2,t},$$

over  $u_1, u_2 \in U$ , with  $A_k > 0, B_k > 0$  for  $k = 1, 2$ ,  $C > 0$ ,  $D > 0$  constants such that  $C, D \in (0, 1)$ , and the subscripts denote time steps. The control pair is denoted by the vectors  $u_1 =$



$(u_{1,0}, u_{1,1}, \dots, u_{1,T-1})$  and  $u_2 = (u_{2,0}, u_{2,1}, \dots, u_{2,T-1})$ , respectively. The cost terms  $A_1 u_{1,t}^2$  and  $B_1 u_{2,t}^2$  have a quadratic dependence on the optimal control pair  $u_{1,t}$  and  $u_{2,t}$ , respectively. This quadratic dependence accounts for nonlinear increases in the translocation costs of the reserve populations as the proportion translocated at a given time step increases. Also, the cost terms  $A_2 u_{1,t}$  and  $B_2 u_{2,t}$  have linear dependence on the optimal control pair  $u_{1,t}$  and  $u_{2,t}$ , respectively. The linear dependence accounts for linear increases in the translocation costs as the proportion translocated at each time step increases. Hence, the objective functional (9) accounts for both linear and nonlinear cost increases.

The set of optimal control pairs is given by

$$(10) \quad U = \{(u_1, u_2) | u_i = (u_{i,0}, u_{i,1}, \dots, u_{i,T-1}) \mid 0 \leq u_{j,t} \leq \Gamma_i, \quad j = 1, 2, \quad i = 1, 2, \quad t = 0, 1, \dots, T-1\},$$

where  $\Gamma_i \in (0, 1)$  for  $i = 1, 2$ , is the maximum control efforts for the control pairs  $u_{1,t}$  and  $u_{2,t}$ , respectively.

We will employ the generalization of Pontryagin's Maximum Principle [48, 49] for the optimal control of discrete-time state systems to obtain the necessary conditions satisfying the optimality system. The method appends the discrete-time states system (6) to the objective functional maximization by utilizing adjoint functions. Pontryagin's Maximum Principle optimizes a system of discrete difference equations, including state and adjoint equations, and provides optimal control characterizations. The adjoint technique provides the gradient of the objective functional (cost function), which is necessary for maximizing. Also, the state system has initial conditions, whereas the adjoint system has final time boundary conditions.

Now, we apply the discrete version of Pontryagin's Maximum Principle [48, 49] for optimal control problems and form the Hamiltonian function as

$$(11) \quad \begin{aligned} H_t = & -A_1 u_{1,t}^2 - A_2 u_{1,t} - B_1 u_{2,t}^2 - B_2 u_{2,t} \\ & + \lambda_{1,t+1} \{x_{1,t} + r_1 x_{1,t} (1 - x_{1,t})(x_{1,t} - a) - \phi_1 x_{1,t} y_{1,t} + \rho_1 u_{1,t} x_{2,t}\} \\ & + \lambda_{2,t+1} \{y_{1,t} + r_2 y_{1,t} (1 - y_{1,t})(y_{1,t} - b) - \phi_2 x_{1,t} y_{1,t} + \rho_2 u_{2,t} y_{2,t}\} \\ & + \lambda_{3,t+1} \{x_{2,t} + r_3 x_{2,t} (1 - x_{2,t})(x_{2,t} - c) - u_{1,t} x_{2,t}\} \\ & + \lambda_{4,t+1} \{y_{2,t} + r_4 y_{2,t} (1 - y_{2,t})(y_{2,t} - d) - u_{2,t} y_{2,t}\}, \end{aligned}$$

where  $t = 1, 2, \dots, T$ .

In the next theorem, the Hamiltonian function (11) will be used to obtain the necessary conditions satisfying the optimal augmentation model (6) and objective functional (9) which will further aid in achieving the optimality system of our problem.

**Theorem 3.1.** *Given the vector of an optimal control pair  $u_1^*, u_2^* \in U$ , where  $(u_1^* = (u_{1,0}^*, u_{1,1}^*, \dots, u_{1,T-1}^*)$  and  $u_2 = (u_{2,0}^*, u_{2,1}^*, \dots, u_{2,T-1}^*)$  with the corresponding states solutions  $x_1^* = (x_{1,0}^*, x_{1,1}^*, \dots, x_{1,T}^*)$ ,  $y_1^* = (y_{1,0}^*, y_{1,1}^*, \dots, y_{1,T}^*)$ ,  $x_2^* = (x_{2,0}^*, x_{2,1}^*, \dots, x_{2,T}^*)$  and  $y_2^* = (y_{2,0}^*, y_{2,1}^*, \dots, y_{2,T}^*)$ , then from system (6) and objective functional (9), there exists adjoint functions  $\lambda_1 = (\lambda_{1,0}, \lambda_{1,1}, \dots, \lambda_{1,T})$ ,  $\lambda_2 = (\lambda_{2,0}, \lambda_{2,1}, \dots, \lambda_{2,T})$ ,  $\lambda_3 = (\lambda_{3,0}, \lambda_{3,1}, \dots, \lambda_{3,T})$  and  $\lambda_4 = (\lambda_{4,0}, \lambda_{4,1}, \dots, \lambda_{4,T})$  satisfying the adjoint equations and the transversality boundary conditions*

$$(12) \quad \left\{ \begin{array}{l} \lambda_{1,t} = \lambda_{1,t+1} + r_1 [2(1+a)x_{1,t}^* - 3(x_{1,t}^*)^2 - a] \lambda_{1,t+1} - (\phi_1 \lambda_{1,t+1} + \phi_2 \lambda_{2,t+1}) y_{1,t}^*, \\ \lambda_{1,T} = 1, \\ \lambda_{2,t} = \lambda_{2,t+1} + r_2 [2(1+b)y_{1,t}^* - 3(y_{1,t}^*)^2 - b] \lambda_{2,t+1} - (\phi_1 \lambda_{1,t+1} + \phi_2 \lambda_{2,t+1}) x_{1,t}^*, \\ \lambda_{2,T} = 1, \\ \lambda_{3,t} = \lambda_{3,t+1} + r_3 [2(1+c)x_{2,t}^* - 3(x_{2,t}^*)^2 - c] \lambda_{3,t+1} + (\rho_1 \lambda_{1,t+1} - \lambda_{3,t+1}) u_{1,t}^*, \\ \lambda_{3,T} = C, \\ \lambda_{4,t} = \lambda_{4,t+1} + r_3 [2(1+d)y_{2,t}^* - 3(y_{2,t}^*)^2 - d] \lambda_{4,t+1} + (\rho_2 \lambda_{2,t+1} - \lambda_{4,t+1}) u_{2,t}^*, \\ \lambda_{4,T} = D. \end{array} \right.$$

In addition, the characterization of the optimal control pair,  $(u_{1,t}^*, u_{2,t}^*)$  is calculated as

$$(13) \quad \left\{ \begin{array}{l} u_{1,t}^* = \min \left\{ \Gamma_1, \max \left\{ 0, \frac{\rho_1 x_{2,t}^* \lambda_{1,t+1} - x_{2,t}^* \lambda_{3,t+1} - A_2}{2A_1} \right\} \right\}, \\ u_{2,t}^* = \min \left\{ \Gamma_2, \max \left\{ 0, \frac{\rho_2 y_{2,t}^* \lambda_{2,t+1} - y_{2,t}^* \lambda_{4,t+1} - B_2}{2B_1} \right\} \right\}. \end{array} \right.$$

*Proof.* Assuming  $(u_1^* = (u_{1,0}^*, u_{1,1}^*, \dots, u_{1,T-1}^*)$  and  $u_2^* = (u_{2,0}^*, u_{2,1}^*, \dots, u_{2,T-1}^*)$  are the vectors of optimal control pair with the corresponding states solutions  $x_1^* = (x_{1,0}^*, x_{1,1}^*, \dots, x_{1,T}^*)$ ,  $y_1^* = (y_{1,0}^*, y_{1,1}^*, \dots, y_{1,T}^*)$ ,  $x_2^* = (x_{2,0}^*, x_{2,1}^*, \dots, x_{2,T}^*)$  and  $y_2^* = (y_{2,0}^*, y_{2,1}^*, \dots, y_{2,T}^*)$ , then using the discrete version of Pontryagin's Maximum Principle [49, 48] for discrete-time models and the Hamiltonian function (9), we obtain

$$(14) \quad \begin{cases} \lambda_{1,t} = \frac{\partial H_t}{\partial x_{1,t}}, \\ \lambda_{2,t} = \frac{\partial H_t}{\partial y_{1,t}}, \\ \lambda_{3,t} = \frac{\partial H_t}{\partial x_{2,t}}, \\ \lambda_{4,t} = \frac{\partial H_t}{\partial y_{2,t}}, \end{cases}$$

which gives

$$(15) \quad \begin{aligned} \lambda_{1,t} &= \lambda_{1,t+1} + r_1 [2(1+a)x_{1,t}^* - 3(x_{1,t}^*)^2 - a] \lambda_{1,t+1} - (\phi_1 \lambda_{1,t+1} + \phi_2 \lambda_{2,t+1}) y_{1,t}^*, \\ \lambda_{2,t} &= \lambda_{2,t+1} + r_2 [2(1+b)y_{1,t}^* - 3(y_{1,t}^*)^2 - b] \lambda_{2,t+1} - (\phi_1 \lambda_{1,t+1} + \phi_2 \lambda_{2,t+1}) x_{1,t}^*, \\ \lambda_{3,t} &= \lambda_{3,t+1} + r_3 [2(1+c)x_{2,t}^* - 3(x_{2,t}^*)^2 - c] \lambda_{3,t+1} + (\rho_1 \lambda_{1,t+1} - \lambda_{3,t+1}) u_{1,t}^*, \\ \lambda_{4,t} &= \lambda_{4,t+1} + r_3 [2(1+d)y_{2,t}^* - 3(y_{2,t}^*)^2 - d] \lambda_{4,t+1} + (\rho_2 \lambda_{2,t+1} - \lambda_{4,t+1}) u_{2,t}^*, \end{aligned}$$

with the transversality conditions

$$(16) \quad \begin{aligned} \lambda_{1,T} &= 1, \\ \lambda_{2,T} &= 1, \\ \lambda_{3,T} &= C, \\ \lambda_{4,T} &= D. \end{aligned}$$

Moreover, by differentiating the Hamiltonian (11) with respect to the optimal control pairs, we get

$$(17) \quad \begin{aligned} \frac{\partial H_t}{\partial u_{1,t}} &= -2A_1 u_{1,t} + \rho_1 x_{2,t} \lambda_{x_{1,t+1}} - x_{2,t} \lambda_{3,t+1} - A_2 = 0 \quad \text{at } u_{1,t}^*, \\ \frac{\partial H_t}{\partial u_{2,t}} &= -2B_1 u_{2,t} + \rho_2 y_{2,t} \lambda_{y_{1,t+1}} - y_{2,t} \lambda_{4,t+1} - B_2 = 0 \quad \text{at } u_{2,t}^*, \end{aligned}$$

on the interior of the control intervals, which gives

$$(18) \quad \begin{aligned} u_{1,t}^* &= \frac{\rho_1 x_{2,t}^* \lambda_{1,t+1} - x_{2,t}^* \lambda_{3,t+1} - A_2}{2A_1} \\ u_{2,t}^* &= \frac{\rho_2 y_{2,t}^* \lambda_{2,t+1} - y_{2,t}^* \lambda_{4,t+1} - B_2}{2B_1}. \end{aligned}$$

Therefore, the required pairs of optimal control characterizations are obtained in Equation (13).

Hence, the discrete state system (6), the adjoint system (12), and the characterizations of the optimal control pair (13) give the optimality system for the discrete-time competition model with both linear and quadratic cost constants.  $\square$

### 3.2. Objective Functional with State values over time and Quadratic Cost Terms.

We provide another objective functional without considering the payoff terms, but with the state terms over time and quadratic costs terms only. Thus, the objective is to maximize

$$(19) \quad \mathbb{J}(u_1, u_2) = \sum_{t=0}^{T-1} x_{1,t} + y_{1,t} + Px_{2,t} + Qy_{2,t} - E_1 u_{1,t}^2 - E_2 u_{2,t}^2$$

over the control pair  $u_1, u_2 \in U$ , with  $E_k > 0$ , for  $k = 1, 2$ ,  $P > 0$ ,  $Q > 0$  constants such that  $P, Q \in (0, 1)$ .

The control pair is denoted by the vectors  $u_1 = (u_{1,0}, u_{1,1}, \dots, u_{1,T-1})$  and  $u_2 = (u_{2,0}, u_{2,1}, \dots, u_{2,T-1})$ , respectively where the subscripts denote time steps. The cost terms  $E_1 u_{1,t}^2$  and  $E_2 u_{2,t}^2$  have a quadratic dependence on the optimal control pair  $u_{1,t}$  and  $u_{2,t}$ , respectively. This quadratic dependence accounts for nonlinear increases in the translocation costs as the proportion translocated at a given time step increases. Equation (10) gives the set of optimal control pairs. The Hamiltonian function representing the optimal augmentation problem with only a quadratic objective functional defined in this section is given by

$$(20) \quad \begin{aligned} \mathcal{H}_t = & x_{1,t} + y_{1,t} + Px_{2,t} + Qy_{2,t} - E_1 u_{1,t}^2 - E_2 u_{2,t}^2 \\ & + \lambda_{1,t+1} \{x_{1,t} + r_1 x_{1,t}(1 - x_{1,t})(x_{1,t} - a) - \phi_1 x_{1,t} y_{1,t} + \rho_1 u_{1,t} x_{2,t}\} \\ & + \lambda_{2,t+1} \{y_{1,t} + r_2 y_{1,t}(1 - y_{1,t})(y_{1,t} - b) - \phi_2 x_{1,t} y_{1,t} + \rho_2 u_{2,t} y_{2,t}\} \\ & + \lambda_{3,t+1} \{x_{2,t} + r_3 x_{2,t}(1 - x_{2,t})(x_{2,t} - c) - u_{1,t} x_{2,t}\} \\ & + \lambda_{4,t+1} \{y_{2,t} + r_4 y_{2,t}(1 - y_{2,t})(y_{2,t} - d) - u_{2,t} y_{2,t}\}. \end{aligned}$$

Using the discrete version of the Hamiltonian function (20), we obtain the adjoint differential equations, transversality conditions, and characterization of optimal control pairs satisfying the discrete-time optimal augmentation model (6) and quadratic objective functional (19).

Now from

$$(21) \quad \begin{cases} \lambda_{1,t} = \frac{\partial \mathcal{H}_t}{\partial x_{1,t}}, \\ \lambda_{2,t} = \frac{\partial \mathcal{H}_t}{\partial y_{1,t}}, \\ \lambda_{3,t} = \frac{\partial \mathcal{H}_t}{\partial x_{2,t}}, \\ \lambda_{4,t} = \frac{\partial \mathcal{H}_t}{\partial y_{2,t}}, \end{cases}$$

We obtain the adjoints equations and the boundary conditions for the model with only the quadratic cost of translocation as

$$(22) \quad \begin{aligned} \lambda_{1,t} &= \lambda_{1,t+1} + r_1 [2(1+a)x_{1,t}^* - 3(x_{1,t}^*)^2 - a] \lambda_{1,t+1} - (\phi_1 \lambda_{1,t+1} + \phi_2 \lambda_{2,t+1}) y_{1,t}^* + 1, \\ \lambda_{2,t} &= \lambda_{2,t+1} + r_2 [2(1+b)y_{1,t}^* - 3(y_{1,t}^*)^2 - b] \lambda_{2,t+1} - (\phi_1 \lambda_{1,t+1} + \phi_2 \lambda_{2,t+1}) x_{1,t}^* + 1, \\ \lambda_{3,t} &= \lambda_{3,t+1} + r_3 [2(1+c)x_{2,t}^* - 3(x_{2,t}^*)^2 - c] \lambda_{3,t+1} + (\rho_1 \lambda_{1,t+1} - \lambda_{3,t+1}) u_{1,t}^* + P, \\ \lambda_{4,t} &= \lambda_{4,t+1} + r_3 [2(1+d)y_{2,t}^* - 3(y_{2,t}^*)^2 - d] \lambda_{4,t+1} + (\rho_2 \lambda_{2,t+1} - \lambda_{4,t+1}) u_{2,t}^* + Q, \end{aligned}$$

$$(23) \quad \begin{aligned} \lambda_{1,T} &= 0, \\ \lambda_{2,T} &= 0, \\ \lambda_{3,T} &= 0, \\ \lambda_{4,T} &= 0. \end{aligned}$$

Furthermore, differentiating the Hamiltonian (20) with respect to the optimal control pairs

$$(24) \quad \begin{aligned} \frac{\partial \mathcal{H}_t}{\partial u_{1,t}} &= 0 \quad \text{at } u_{1,t}^*, \\ \frac{\partial H_t}{\partial u_{2,t}} &= 0 \quad \text{at } u_{2,t}^*, \end{aligned}$$

we then obtain the new characterization of the optimal control pair as

$$(25) \quad \begin{aligned} u_{1,t}^* &= \min \left\{ \Gamma_1, \max \left\{ 0, \frac{\rho_1 x_{2,t}^* \lambda_{1,t+1} - x_{2,t}^* \lambda_{3,t+1}}{2E_1} \right\} \right\}, \\ u_{2,t}^* &= \min \left\{ \Gamma_2, \max \left\{ 0, \frac{\rho_2 y_{2,t}^* \lambda_{2,t+1} - y_{2,t}^* \lambda_{4,t+1}}{2E_2} \right\} \right\}. \end{aligned}$$

#### 4. NUMERICAL SIMULATIONS AND DISCUSSIONS

We will employ the discrete generalization of the forward-backward sweep method to solve the optimality systems using MATLAB software. Using initial guesses of the vector of optimal control pairs ( $u_1 = (u_{1,0}, u_{1,1}, \dots, u_{1,T-1})$ ) and ( $u_2 = (u_{2,0}, u_{2,1}, \dots, u_{2,T-1})$ ) and the initial conditions  $x_{1,0} > 0, y_{1,0} > 0, x_{2,0} > 0, y_{2,0} > 0$ , the state vectors ( $x_1 = (x_{1,0}, x_{1,1}, \dots, x_{1,T})$ ), ( $y_1 = (y_{1,0}, y_{1,1}, \dots, y_{1,T})$ ), ( $x_2 = (x_{2,0}, x_{2,1}, \dots, x_{2,T})$ ) and ( $y_2 = (y_{2,0}, y_{2,1}, \dots, y_{2,T})$ ) are solved forward in time. Then the adjoint variables  $\lambda_1 = (\lambda_{1,0}, \lambda_{1,1}, \dots, \lambda_{1,T})$ ,  $\lambda_2 = (\lambda_{2,0}, \lambda_{2,1}, \dots, \lambda_{2,T})$ ,  $\lambda_3 = (\lambda_{3,0}, \lambda_{3,1}, \dots, \lambda_{3,T})$  and  $\lambda_4 = (\lambda_{4,0}, \lambda_{4,1}, \dots, \lambda_{4,T})$  are solved backwards in time using transversality conditions and the newly found controls. Finally, the optimal controls are updated from the characterization of the optimal controls and the adjoint and state variables, and this process repeats until the successive iterate of the control value is sufficiently small [49].

In the simulations, we set the Allee constants  $a = b = c = d = 0.35$  and the initial conditions  $x_{1,0} = 0.30 < a, y_{1,0} = 0.25 < b, x_{2,0} = 0.95 > c$ , and  $y_{2,0} = 0.75 > d$ . The rest of the parameter values can be found in the captions of each figure. First, we will simulate the model with both linear and quadratic costs of translocating individuals before considering the model with only the quadratic cost of translocating individuals.

In the numerical results, we will begin with the plots of the model using baseline parameters. Again, the impacts of the cost constraints on the model will be discussed. We will examine the effect of the competition factors on the model. Finally, the results of varying the augmentation coefficients will be presented. In addition to the above scenarios, the objective functional values will be computed for each simulation. Optimal control values indicating the percentage weights of the reserve species translocated at each time step will be discussed through the simulations.

Throughout the simulations, the plots of the reserve and target populations with optimal controls are indicated in blue and red, respectively, while the plots of these populations without controls are indicated in black. One can observe that the endangered or target species population levels (plots in black) are decreasing towards extinction as time progresses; however, the reserve species population levels are growing well and are viable sources for harvesting individuals for augmentation. Again, the reserve population levels with optimal controls (plots in blue) show population levels higher than the threshold for growth throughout the entire simulation.

#### 4.1. Simulation of the Discrete-time Competition Model with both Linear and Quadratic Cost Constants.

We present the numerical results of the discrete-time optimal control of the competition model, considering both linear and quadratic costs of translocating individuals from reserve environments to target regions. Figure 1 is based on the set of baseline values. The plots of the states and the plots of the corresponding optimal controls in Figure 1 indicate that the endangered and the reserve populations levels are above the minimum threshold for growth. The optimal control pair values

$$(26) \quad \begin{aligned} u_{1,t} &= [0.055, 0.046, 0.045, 0.046, 0.050, 0.056, 0.069, 0.120], \\ u_{2,t} &= [0.059, 0.069, 0.076, 0.081, 0.084, 0.089, 0.103, 0.144], \end{aligned}$$

show that for the optimal control  $u_{1,t}$ , about 5.4% of the reserve population  $x_{2,t}$  are translocated at time steps  $t = 0$ , about 4.6% of the reserve population  $x_{2,t}$  are translocated at time steps  $t = 1, 3$ , and about 4.4%, 5.6%, 6.9%, and 12% individuals are translocated at time steps  $t = 2, 4, 5, 6$ , and 7, respectively. Again, the values of the optimal control  $u_{2,t}$  indicate that about 5.9%, 6.9%, 7.6%, 8.1%, 8.4%, 8.9%, 10.3% and 14.4% of the reserve population  $y_{2,t}$  are translocated at time steps  $t = 0, 1, 2, 3, 4, 5, 6$ , and 7, respectively. Furthermore, the values of the objective functional are  $\mathbf{J}(0,0) = 0.7850$  and  $\mathbf{J}(u_1^*, u_2^*) = 1.3234$ ; that is, translocation of individuals at the given time steps gives a 69% higher objective functional value than without moving reserve species. Since the target or the endangered population levels are all above the threshold for growth (i.e.,  $x_{1,0} < a, y_{1,0} < b$ ), their population will be able to grow after the augmentation effort.

In Figure 2, the cost constants  $A_1$  and  $B_1$  are increased from 3 to 30 and 2 to 25, respectively. With this, the endangered population levels were below the threshold for growth by the final time  $T = 8$  due to high cost coefficients. As a result, the reserve population levels were much higher than those in Figure 1 because a few individuals can be translocated with these high cost coefficients. The values of the optimal control pairs in this case are

$$(27) \quad \begin{aligned} u_{1,t} &= [0.0148, 0.0152, 0.0155, 0.0156, 0.0158, 0.0160, 0.0158, 0.0130], \\ u_{2,t} &= [0.0066, 0.0086, 0.0105, 0.0122, 0.0135, 0.0145, 0.0150, 0.0134]. \end{aligned}$$

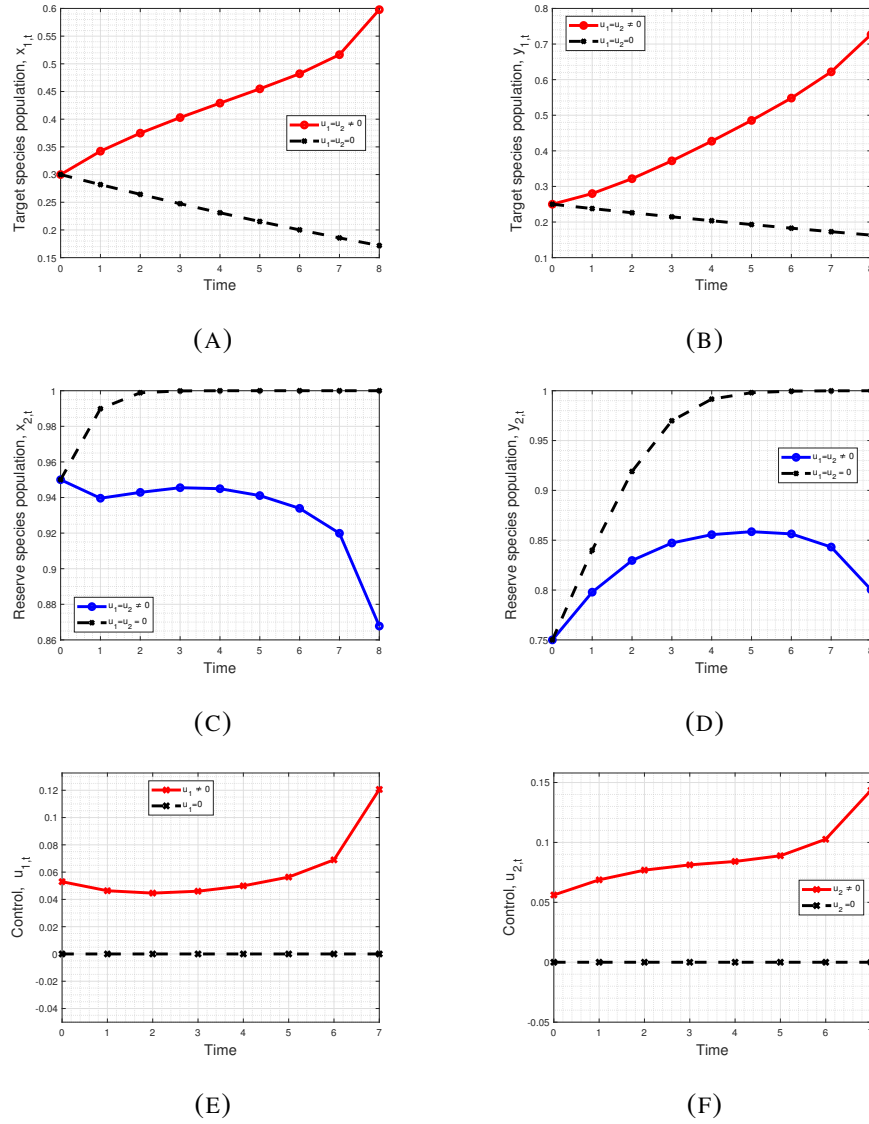


FIGURE 1. Simulations of the discrete-time competition model of species augmentation using the baseline parameter values:  $A_1 = 3$ ,  $A_2 = 0.15$ ,  $B_1 = 2$ ,  $B_2 = 0.1$ ,  $\rho_1 = 1.2$ ,  $\rho_2 = 1.0$ ,  $\phi_1 = 0.2$ ,  $\phi_2 = 0.1$ ,  $C = 0.25$ ,  $D = 0.2$ ,  $r_1 = 0.3$ ,  $r_2 = 0.25$ ,  $r_3 = 1.4$ , and  $r_4 = 1.2$ . The corresponding objective functional values are  $J(0,0) = 0.7850$  (without controls), and  $J(u_1^*, u_2^*) = 1.3234$  (with optimal controls). Optimal control pair values are  $u_1 = [0.055, 0.046, 0.045, 0.046, 0.050, 0.056, 0.069, 0.12]$ ,  $u_2 = [0.059, 0.069, 0.076, 0.081, 0.084, 0.089, 0.103, 0.144]$ .



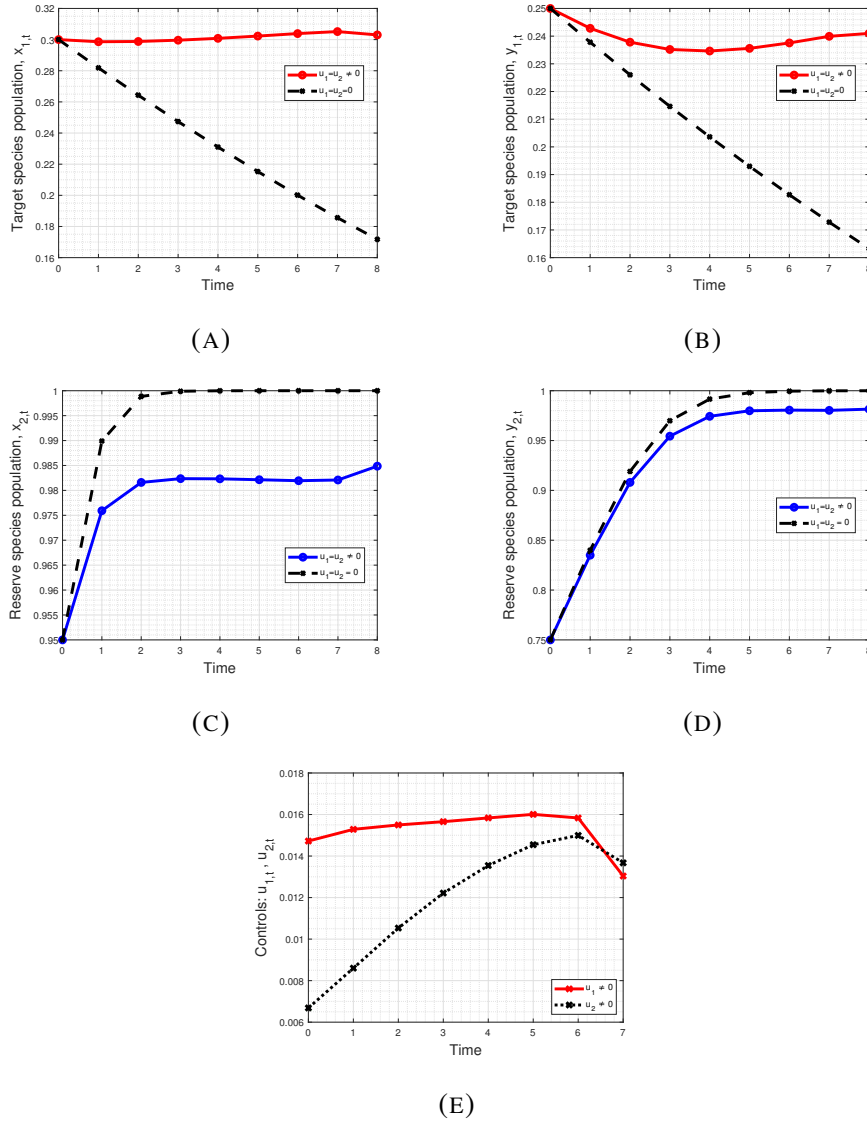


FIGURE 2. Simulations of the discrete-time competition model of species augmentation using the parameter values:  $A_1 = 30$ ,  $A_2 = 0.15$ ,  $B_1 = 25$ ,  $B_2 = 0.1$ ,  $\rho_1 = 1.2$ ,  $\rho_2 = 1.0$ ,  $\phi_1 = 0.2$ ,  $\phi_2 = 0.1$ ,  $C = 0.25$ ,  $D = 0.2$ ,  $r_1 = 0.3$ ,  $r_2 = 0.25$ ,  $r_3 = 1.4$ , and  $r_4 = 1.2$ . The corresponding objective functional values are  $\mathbf{J}(0,0) = 0.7850$  (without controls), and  $\mathbf{J}(u_1^*, u_2^*) = 0.8733$  (with optimal controls). Optimal control pair values are  $u_1 = [0.0148, 0.0152, 0.0155, 0.0156, 0.0158, 0.0160, 0.0158, 0.0130]$ ,  $u_2 = [0.0066, 0.0086, 0.0105, 0.0122, 0.0135, 0.0145, 0.0150, 0.0134]$ .

The optimal control  $u_{1,t}$  values in Equation (27) illustrate that about 1.48%, 1.55%, 1.56%, 1.58%, 1.6%, 1.58% and 1.3% are translocated at the time steps  $t = 0, 1, 2, 3, 4, 5, 6, 7$ , respectively. Also, the values of the optimal optimal control  $u_{2,t}$  in Equation (27) indicate that at time steps  $t = 0, 1, 2, 3, 4, 5, 6$ , and 7, about 0.66%, 0.86%, 1.05%, 1.22%, 1.35%, 1.45%, 1.5% and 1.34% of the reserve population  $y_{2,t}$  are translocated, respectively. The values of the objective functional are  $\mathbf{J}(0,0) = 0.7850$  and  $\mathbf{J}(u_1^*, u_2^*) = 0.8733$ ; that is, translocation of individuals from the reserve population  $y_{2,t}$  using the baseline values as those in Figure 1 except the cost constants  $A_1 = 30$  and  $B_1 = 25$  gives 11% higher objective functional values than when there is no translocation of individuals. Here, without the augmentation effort, the target populations may not be able to grow after the final time due to the low population levels.

The numerical simulation in Figure 3 was conducted using the baseline values except for  $A_2 = 0$  and  $B_2 = 0$ . In this parameter setting, the result depicts an increase of the target and the reserve population levels at the end of the horizon as compared to Figure 1. That is, at the final time step  $T = 8$ , the target populations  $x_{1,t}$  and  $y_{1,t}$  show a population levels of 0.69 and 1.21, respectively, due to setting the constants  $A_2 = 0$  and  $B_2 = 0$ . Similarly, the reserve populations  $x_{2,t}$  and  $y_{2,t}$  indicate population levels of 1.18 and 1.25, respectively, which are all above the threshold for growth. The optimal control pair values obtained are

$$(28) \quad \begin{aligned} u_{1,t} &= [0.062, 0.055, 0.053, 0.054, 0.057, 0.063, 0.770, 0.144], \\ u_{2,t} &= [0.068, 0.077, 0.084, 0.087, 0.090, 0.096, 0.114, 0.165]. \end{aligned}$$

The values of  $u_{1,t}$  indicate that at time steps  $t = 0, 1, 2, 3, 4, 5, 6, 7$ , about 6.2%, 5.5%, 5.3%, 5.4%, 5.7%, 6.3%, 7.7% and 14.4% individuals are translocated, respectively. Moreover,  $u_{2,t}$  values show that about 6.8%, 7.7%, 8.4%, 8.7%, 9%, 14%, 9.6% and 16.5% individuals are moved from the reserve to the target region at time steps  $t = 0, 1, 2, 3, 4, 6$ , and 7, respectively. The objective functional values  $\mathbf{J}(0,0) = 0.7850$ , and  $\mathbf{J}(u_1^*, u_2^*) = 1.4930$ ; indicating 90% higher objective functional values with optimal controls than when there are no optimal controls. Again, with the population levels of 6.6 and 7.8 for the target populations  $x_{1,t}$  and  $y_{1,t}$ , respectively, they will be able to grow after the time horizon without additional augmentation effort.

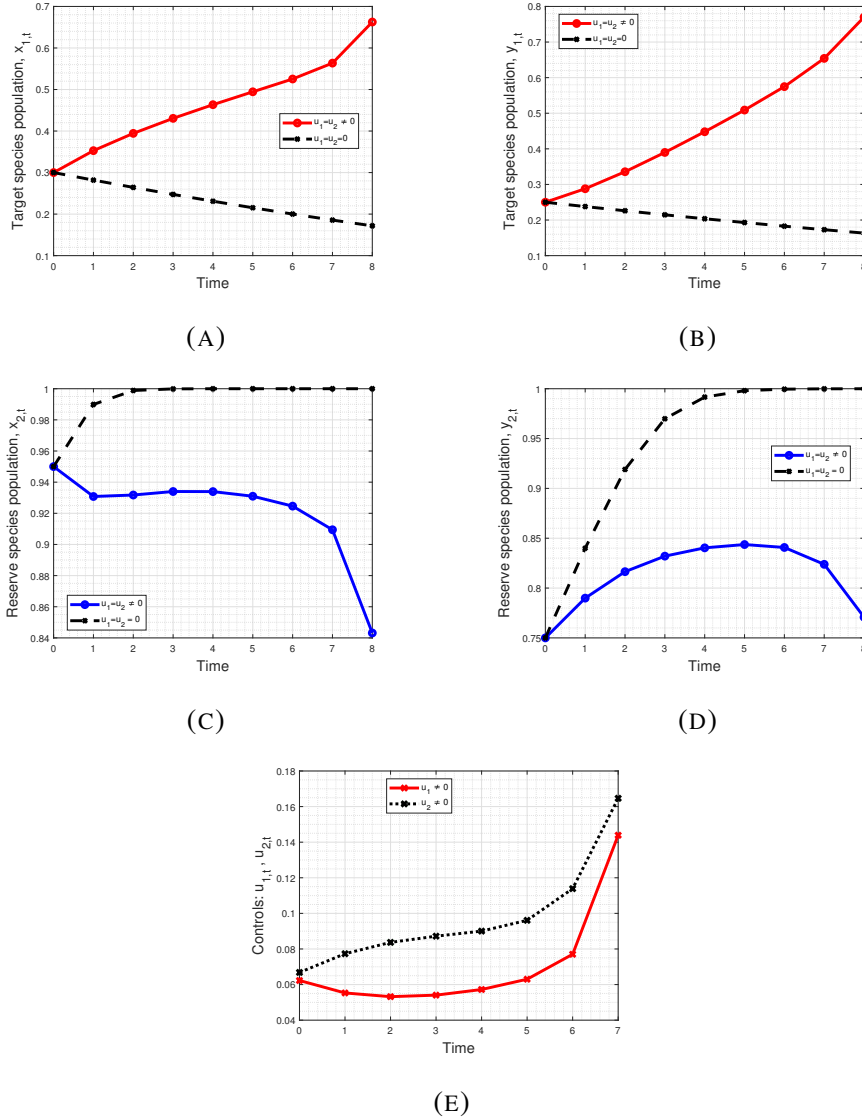


FIGURE 3. Simulations of the discrete-time competition model of species augmentation using the parameter values:  $A_1 = 3$ ,  $A_2 = 0$ ,  $B_1 = 2$ ,  $B_2 = 0$ ,  $\rho_1 = 1.4$ ,  $\rho_2 = 1.2$ ,  $\phi_1 = 0.2$ ,  $\phi_2 = 0.1$ ,  $C = 0.25$ ,  $D = 0.2$ ,  $r_1 = 0.3$ ,  $r_2 = 0.25$ ,  $r_3 = 1.4$ , and  $r_4 = 1.2$ . The corresponding objective functional values are  $\mathbf{J}(0,0) = 0.7850$  (without controls), and  $\mathbf{J}(u_1^*, u_2^*) = 1.4930$  (with optimal controls). Optimal control pair values are  $u_1 = [0.062, 0.055, 0.053, 0.054, 0.057, 0.063, 0.77, 0.144]$ ,  $u_2 = [0.068, 0.077, 0.084, 0.087, 0.090, 0.096, 0.114, 0.165]$ .

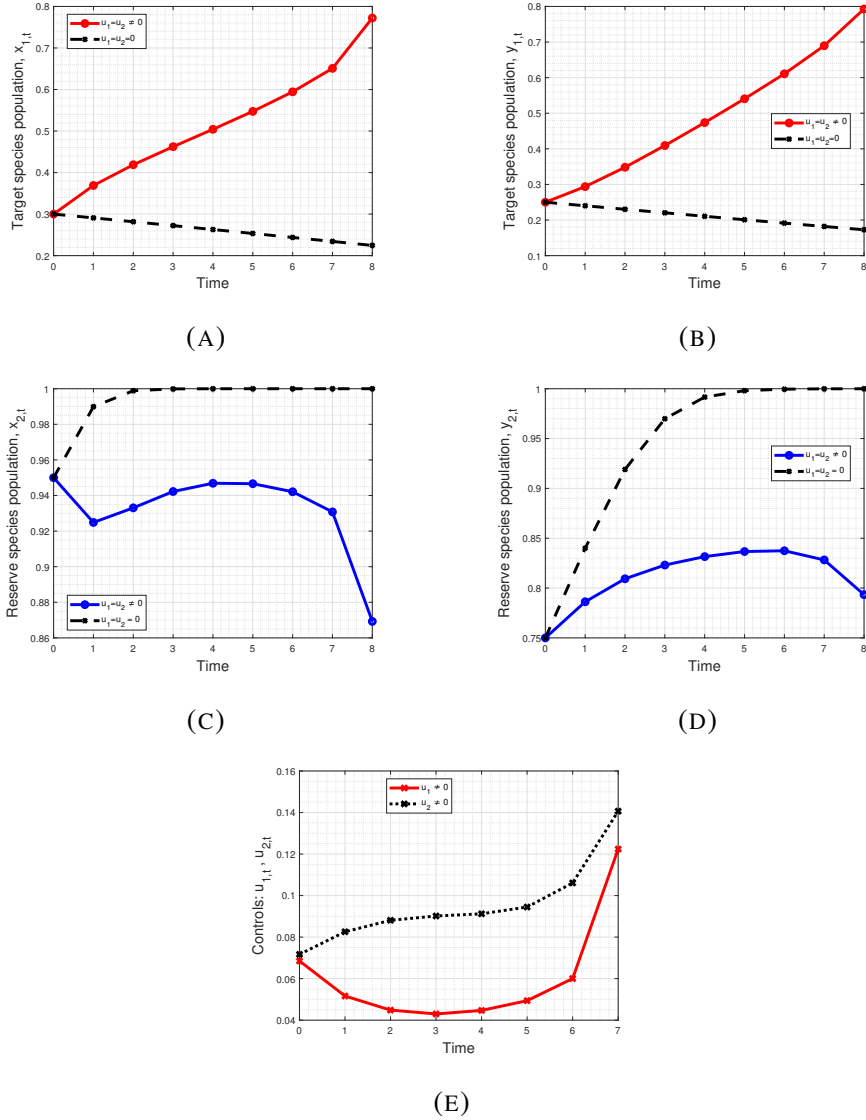


FIGURE 4. Simulations of the discrete-time competition model of species augmentation using the parameter values:  $A_1 = 3$ ,  $A_2 = 0.15$ ,  $B_1 = 2$ ,  $B_2 = 0.1$ ,  $\rho_1 = 1.2$ ,  $\rho_2 = 1.0$ ,  $\phi_1 = 0.08$ ,  $\phi_2 = 0.07$ ,  $C = 0.25$ ,  $D = 0.2$ ,  $r_1 = 0.3$ ,  $r_2 = 0.25$ ,  $r_3 = 1.4$ , and  $r_4 = 1.2$ . The corresponding objective functional values are  $J(0,0) = 0.8472$  (without controls), and  $J(u_1^*, u_2^*) = 1.5371$  (with optimal controls). Optimal control pair values are  $u_1 = [0.069, 0.052, 0.045, 0.043, 0.045, 0.049, 0.060, 0.122]$ ,  $u_2 = [0.072, 0.083, 0.088, 0.090, 0.091, 0.094, 0.106, 0.141]$ .

To examine the impact of the competition factor, Figure 4 illustrates the plots of the states and the plots of the corresponding optimal controls using the same parameter values as those in Figure 1 except reducing the competition coefficients  $\phi_1$  and  $\phi_2$  from 0.20 and 0.10 to 0.08 and 0.07, respectively. In this parameter set, the target populations  $x_{1,t}$  and  $y_{1,t}$  population levels have increased to 0.78 and 0.80, respectively, which are all above the threshold for growth. In the same way, the reserve populations  $x_{2,t}$  and  $y_{2,t}$  population levels are 0.87 and 0.79, respectively, which are above the threshold for growth. Again, the optimal control pair values obtained via the simulation are

$$(29) \quad \begin{aligned} u_{1,t} &= [0.069, 0.052, 0.045, 0.043, 0.045, 0.049, 0.060, 0.122, \\ u_{2,t} &= [0.072, 0.083, 0.088, 0.090, 0.091, 0.094, 0.106, 0.141], \end{aligned}$$

showing that for optimal control  $u_{1,t}$ , about 6.9%, 5.2%, 4.5%, 4.3%, 4.5%, 4.9%, 6% and 12.2% individuals are harvested and translocated at time steps  $t = 0, 1, 2, 3, 4, 5, 6$ , and  $t = 7$ , respectively. Again, for the optimal control  $u_{2,t}$ , about 7.2%, 8.3%, 8.8%, 9%, 9.1%, 9.4%, 10.6% and 14.1% at time steps  $t = 0, 1, 2, 3, 4, 5, 6$ , and  $t = 7$ , respectively. The objective functional values  $\mathbf{J}(0, 0) = 0.8472$ , and  $\mathbf{J}(u_1^*, u_2^*) = 1.5371$  differ by 81%.

In Figure 5, we examined the impact of the augmentation coefficients,  $\rho_1$  and  $\rho_2$  by reducing their values from 1.2 and 1.0 to 0.35 and 0.30, respectively. With these parameter settings, the target populations exhibit a decline in population levels, indicating possible extinction of the target species. The reserve species population levels are very high, close to those without optimal controls. The pair of optimal control values

$$(30) \quad \begin{aligned} u_{1,t} &= [0.025, 0.028, 0.029, 0.030, 0.030, 0.029, 0.024, 0], \\ u_{2,t} &= [0.006, 0.014, 0.021, 0.026, 0.030, 0.031, 0.026, 0], \end{aligned}$$

show that about 2.5% of reserve population  $x_{2,t}$  are translocated at the time step  $t = 0$ , about 2.8% of reserve population  $x_{2,t}$  are translocated at the time step  $t = 1$ , about 2.9% are translocated at time step  $t = 2, 5$ , about 3% are translocated at time step  $t = 3, 4$ , 2.4% are translocated at time step  $t = 6$ , and no individual of reserve species  $x_{2,t}$  is translocated at the time step  $t = 7$ . Furthermore, the values of  $u_{2,t}$  illustrate that about 0.6%, 1.4%, 2.1%, 2.6%, 3.0%, 3.1% and 2.6% of the reserve population  $y_{2,t}$  are translocated at the time steps  $t = 0, 1, 2, 3, 4, 5$ , and 6,

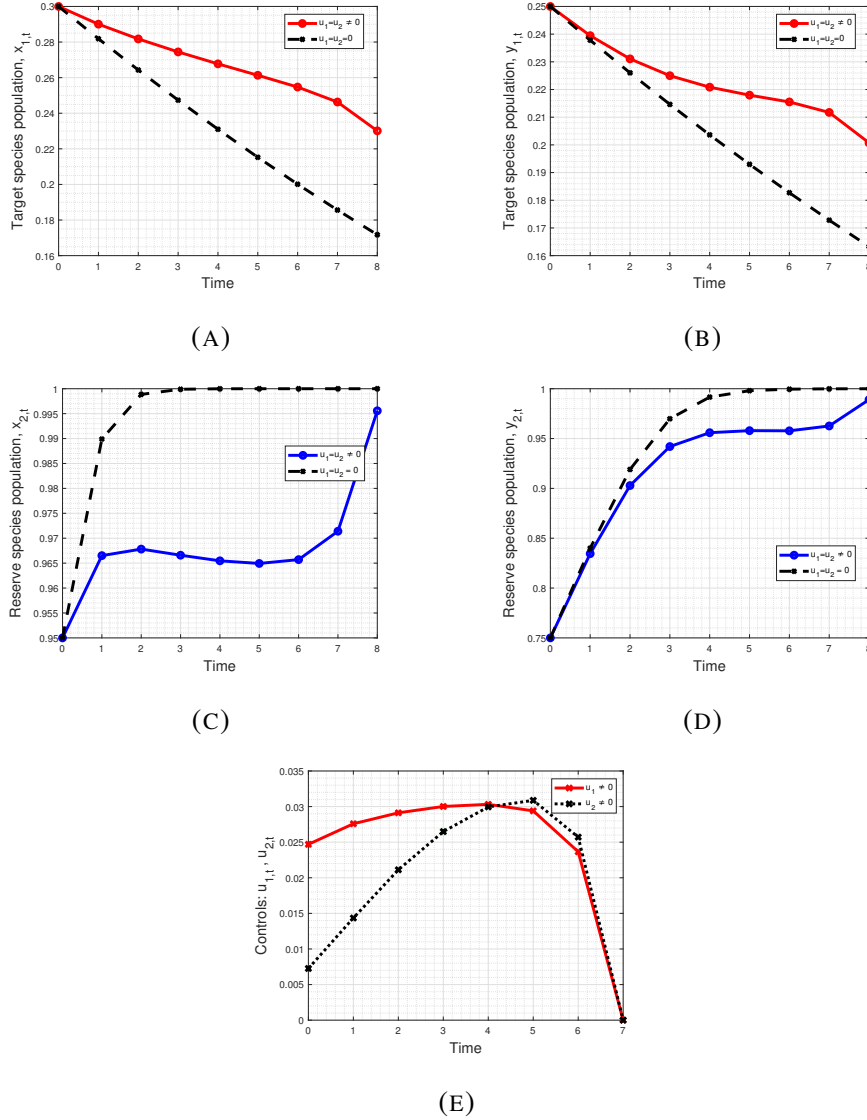


FIGURE 5. Simulations of the discrete-time competition model of species augmentation using the parameter values:  $A_1 = 3$ ,  $A_2 = 0.15$ ,  $B_1 = 2$ ,  $B_2 = 0.1$ ,  $\rho_1 = 0.35$ ,  $\rho_2 = 0.30$ ,  $\phi_1 = 0.2$ ,  $\phi_2 = 0.1$ ,  $C = 0.25$ ,  $D = 0.2$ ,  $r_1 = 0.3$ ,  $r_2 = 0.25$ ,  $r_3 = 1.4$ , and  $r_4 = 1.2$ . The corresponding objective functional values are  $\mathbf{J}(0,0) = 0.7850$  (without controls), and  $\mathbf{J}(u_1^*, u_2^*) = 0.8086$  (with optimal controls). Optimal control pair values are  $u_1 = [0.025, 0.028, 0.029, 0.030, 0.030, 0.029, 0.024, 0]$ ,  $u_2 = [0.006, 0.014, 0.021, 0.026, 0.030, 0.031, 0.026, 0]$ .

respectively. No individual is translocated at time step  $t = 7$ . Moreover, the values of objective functional  $\mathbf{J}(0,0) = 0.7850$ , and  $\mathbf{J}(u_1^*, u_2^*) = 0.8086$  differ by only 3%.

#### 4.2. Simulation of the Discrete-time Competition Model with Objective Functional with State Values over time and Only Quadratic Cost Constants.

In the subsequent section, the simulation of the discrete-time competition model is generated by considering the objective functional (19). Figure 6 gives the baseline parameters. As observed in Figure 6, without optimal controls, the endangered / target populations  $x_{1,t}$  and  $y_{1,t}$  levels are declining whilst the reserve populations are growing well, showing viable sources for harvesting individuals for augmentation. However, with optimal controls, the target populations  $x_{1,t}$  and  $y_{1,t}$  are growing well with population levels of 0.70 and 0.57, respectively, at the final time  $T = 8$ . This represents that the target populations  $x_{1,t}$  and  $y_{1,t}$  will be able to sustain their growth after the augmentation period. The optimal control pair values

$$(31) \quad \begin{aligned} u_{1,t} &= [0.28, 0.20, 0.18, 0.16, 0.14, 0.11, 0.06, 0.00], \\ u_{2,t} &= [0.22, 0.21, 0.19, 0.17, 0.13, 0.10, 0.05, 0.00], \end{aligned}$$

indicate that about 28%, 20%, 18%, 16%, 14%, 11% and 6% individuals of the reserve population  $x_{2,t}$  are translocated to augment the declining population  $x_{1,t}$  at time steps  $t = 0, 1, 2, 3, 4, 5$  and 6, respectively. No individual is translocated at  $t = 7$ . Similarly, about 22%, 21%, 19%, 17%, 13%, 10% and 5% individuals of the reserve population  $y_{2,t}$  are translocated to augment the declining population  $y_{1,t}$  at time steps  $t = 0, 1, 2, 3, 4, 5$  and 6, respectively. No individual is translocated at  $t = 7$ . In addition, Figure 6 gives objective functional values  $\mathbb{J}(0,0) = 3.9223$ , and  $\mathbb{J}(u_1^*, u_2^*) = 7.8439$ ; indicating about 100% higher objective functional value with optimal controls than without optimal controls.

In Figure 7, the cost constants  $E_1$  and  $E_2$  are increased from 5 and 4 to 75 and 60, respectively. With these changes in the cost constants, the endangered/target populations  $x_{1,t}$  and  $y_{1,t}$  population levels are 0.32 and 0.24, respectively, by the final time  $T = 8$ , which are all less than the minimum threshold for growth ( $a = b = 0.35$ ). Due to the high cost of augmentation, few individuals can be translocated, resulting in high population levels for the reserve species. This

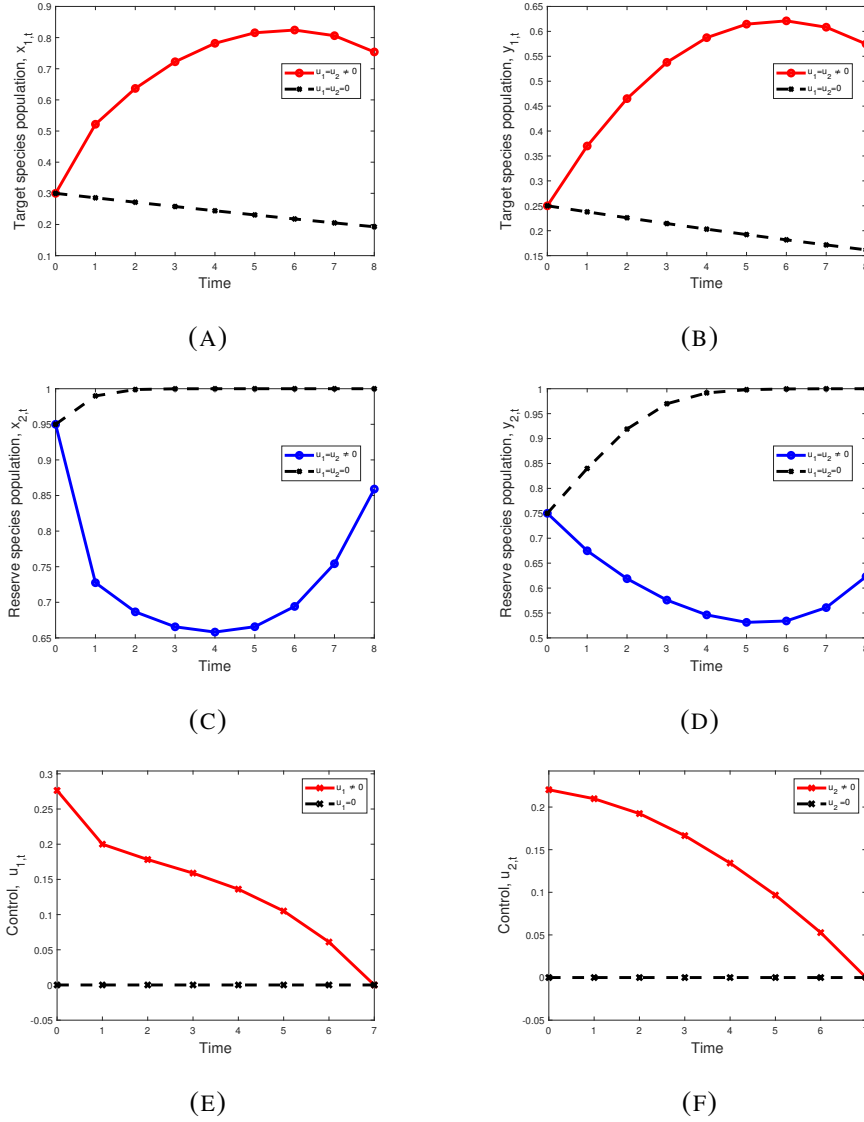


FIGURE 6. Simulations of the discrete-time competition model of species augmentation using the baseline parameter values:  $E_1 = 5$ ,  $E_2 = 4$ ,  $P = 0.02$ ,  $Q = 0.01$ ,  $\rho_1 = 0.90$ ,  $\rho_2 = 0.80$ ,  $\phi_1 = 0.15$ ,  $\phi_2 = 0.10$ ,  $r_1 = 0.30$ ,  $r_2 = 0.25$ ,  $r_3 = 1.40$ ,  $r_4 = 1.20$ . The corresponding objective functional values are  $\mathbb{J}(0,0) = 3.9223$  (without controls), and  $\mathbb{J}(u_1^*, u_2^*) = 7.8439$  (with optimal controls). Optimal control pair values are  $u_1 = [0.28, 0.20, 0.18, 0.16, 0.14, 0.11, 0.06, 0.00]$ ,  $u_2 = [0.22, 0.21, 0.19, 0.17, 0.13, 0.10, 0.05, 0.00]$ .



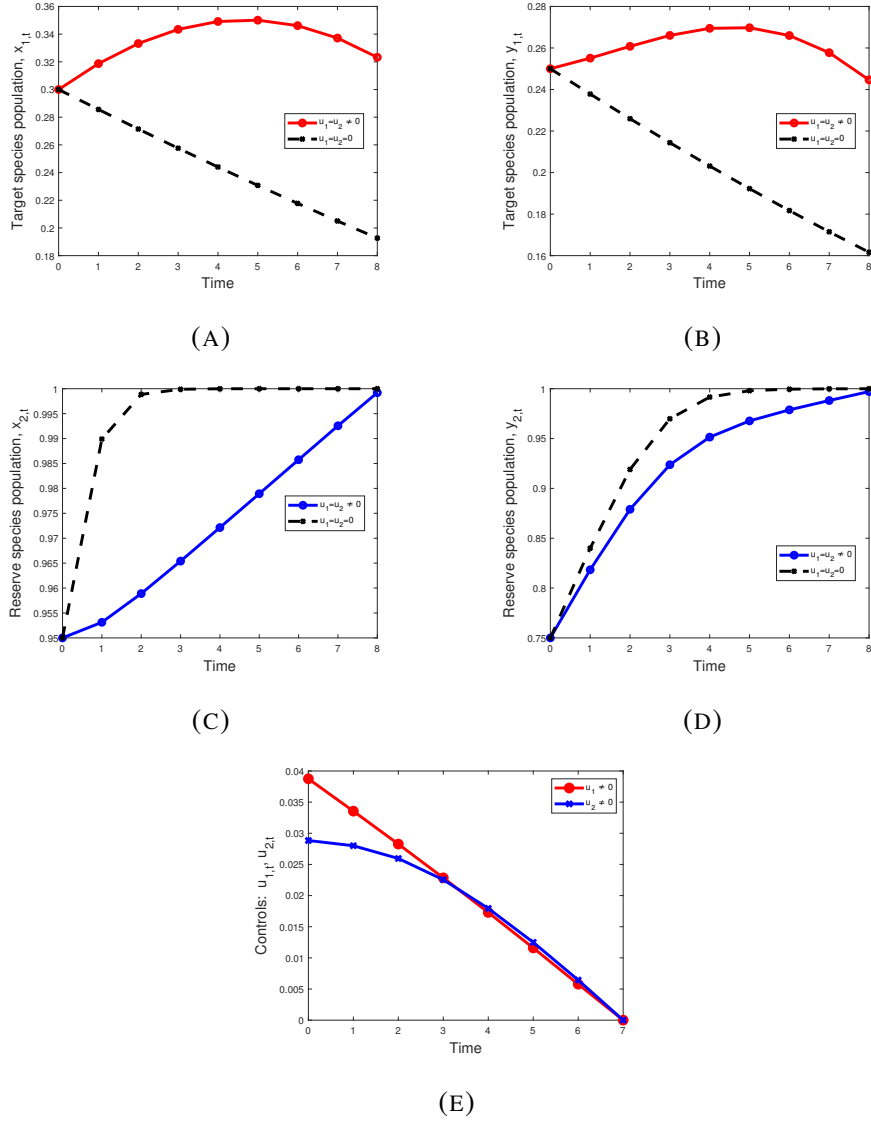


FIGURE 7. Simulations of the discrete-time competition model of species augmentation using parameter values:  $E_1 = 75$ ,  $E_2 = 60$ ,  $P = 0.02$ ,  $Q = 0.01$ ,  $\rho_1 = 0.90$ ,  $\rho_2 = 0.80$ ,  $\phi_1 = 0.15$ ,  $\phi_2 = 0.10$ ,  $r_1 = 0.30$ ,  $r_2 = 0.25$ ,  $r_3 = 1.40$ ,  $r_4 = 1.20$ . The corresponding objective functional values are  $\mathbb{J}(0,0) = 3.9223$  (without controls), and  $\mathbb{J}(u_1^*, u_2^*) = 4.4711$  (with optimal controls). Optimal control pair values are  $u_1 = [0.039, 0.034, 0.028, 0.023, 0.017, 0.012, 0.006, 0.00]$ ,  $u_2 = [0.029, 0.028, 0.026, 0.023, 0.018, 0.012, 0.006, 0.00]$ .

result suggests that the target species will be unable to grow without effort after the augmentation period due to high costs. The values of optimal control pairs are

$$(32) \quad \begin{aligned} u_{1,t} &= [0.039, 0.034, 0.028, 0.023, 0.017, 0.012, 0.006, 0.00], \\ u_{2,t} &= [0.029, 0.028, 0.026, 0.023, 0.018, 0.012, 0.006, 0.00]. \end{aligned}$$

The  $u_{1,t}$  values shows about 3.9%, 3.4%, 2.8%, 2.3%, 1.7%, 1.2% and 6% removed from reserve population  $x_{2,t}$  for augmentation at time steps  $t = 0, 1, 2, 3, 4, 5$ , and 6, respectively. No reserve individual  $x_{2,t}$  is translocated at time step  $t = 7$ . In a similar vein, the  $u_{2,t}$  values represent that about 2.9%, 2.8%, 2.6%, 2.3%, 1.8%, 1.2% and 6% individuals are translocated at time steps  $t = 0, 1, 2, 3, 4, 5$ , and 6, respectively and no reserve individual  $y_{2,t}$  is translocated at time step  $t = 7$ . Again, the values of objective functional  $\mathbb{J}(0,0) = 3.9223$ , and  $\mathbb{J}(u_1^*, u_2^*) = 4.4711$  differ by only 14%.

The graphs in Figure 8 were generated using the same baseline parameters as those in Figure 6 except the competition coefficients  $\phi_1 = 0.80$  and  $\phi_2 = 0.75$ . In these parameter settings, the target population  $x_{1,t}$  shows a very high population level, whilst the target population  $y_{1,t}$  shows a drastic decrease in population level. This illustrates that the competition between species in their ecological habitat can play a crucial role in population extinction. The plots of the reserve populations  $x_{2,t}$  and  $y_{2,t}$  with optimal controls show population levels of 0.77 and 0.95, respectively, at the end of the horizon. The optimal control pair values

$$(33) \quad \begin{aligned} u_{1,t} &= [0.28, 0.24, 0.21, 0.18, 0.14, 0.09, 0.05, 0.00], \\ u_{2,t} &= [0.00, 0.00, 0.00, 0.00, 0.00, 0.08, 0.09, 0.00], \end{aligned}$$

illustrate that about 2.8%, 2.4%, 2.1%, 18%, 14%, 9% and 5% individuals are removed from the reserve population  $x_{2,t}$  for augmentation at time steps  $t = 0, 1, 2, 3, 4, 5$ , and 6, respectively. For the values of the optimal control  $u_{2,t}$ , about 8% individuals are translocated at time step  $t = 5$ , about 9% individuals are translocated at time step  $t = 6$ , and no individual is translocated at time steps  $t = 0, 1, 2, 3, 4$ , respectively. The values of the objective functional are  $\mathbb{J}(0,0) = 2.6173$ , and  $\mathbb{J}(u_1^*, u_2^*) = 5.0664$ ; representing 94% higher objective functional values with optimal controls than when there is no control.

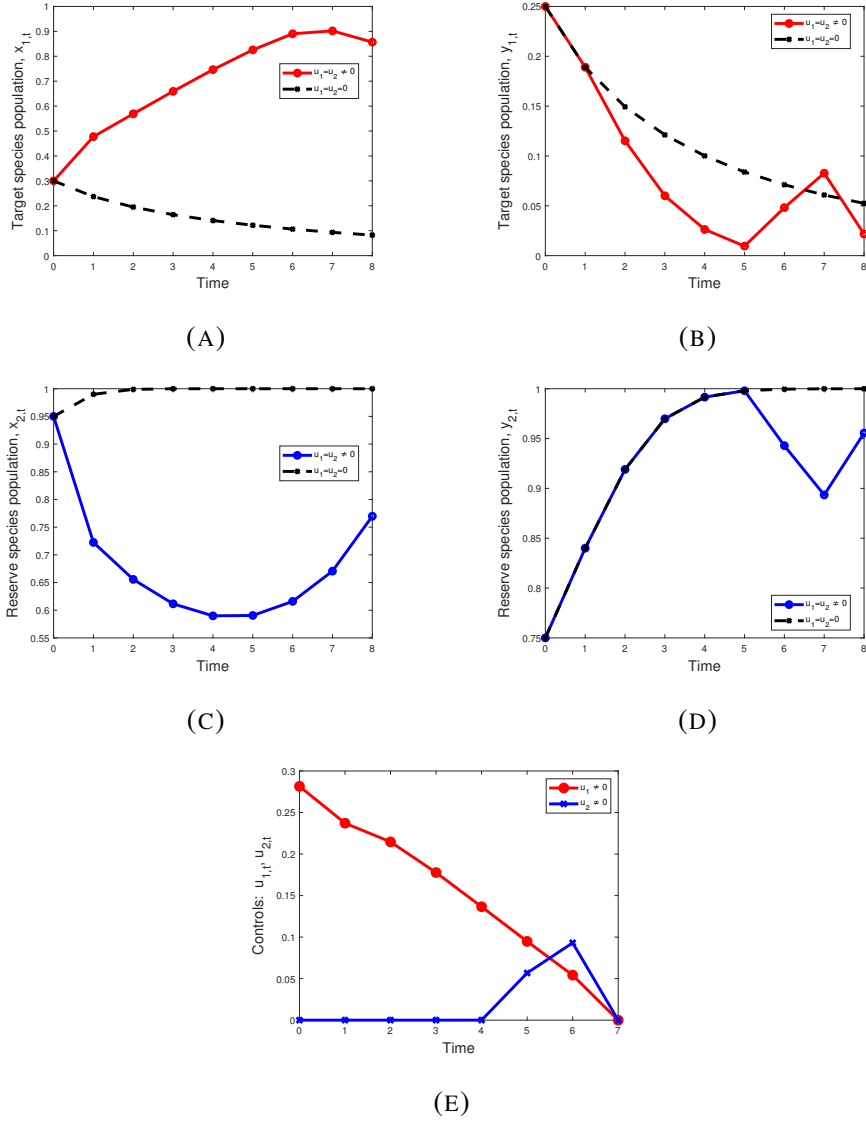


FIGURE 8. Simulations of the discrete-time competition model of species augmentation using parameter values:  $E_1 = 5$ ,  $E_2 = 4$ ,  $P = 0.8$ ,  $Q = 0.7$ ,  $\rho_1 = 0.90$ ,  $\rho_2 = 0.80$ ,  $\phi_1 = 0.80$ ,  $\phi_2 = 0.75$ ,  $r_1 = 0.30$ ,  $r_2 = 0.25$ ,  $r_3 = 1.40$ ,  $r_4 = 1.20$ . The corresponding objective functional values are  $\mathbb{J}(0,0) = 2.6173$  (without controls), and  $\mathbb{J}(u_1^*, u_2^*) = 5.0664$  (with optimal controls). Optimal control pair values are  $u_1 = [0.28, 0.24, 0.21, 0.018, 0.14, 0.09, 0.05, 0.00]$ ,  $u_2 = [0.00, 0.00, 0.00, 0.00, 0.00, 0.08, 0.09, 0.00]$ .

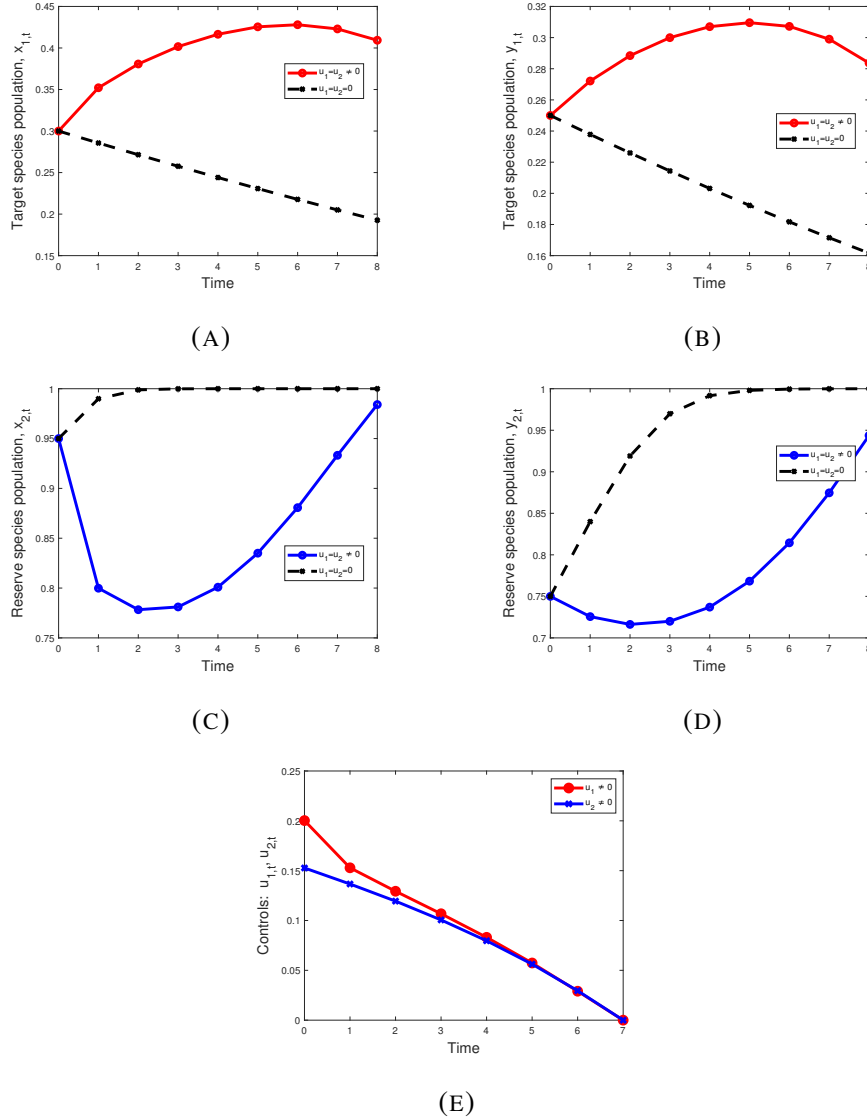


FIGURE 9. Simulations of the discrete-time competition model of species augmentation using the parameter values:  $E_1 = 5$ ,  $E_2 = 4$ ,  $P = 0.02$ ,  $Q = 0.01$ ,  $\rho_1 = 0.35$ ,  $\rho_2 = 0.30$ ,  $\phi_1 = 0.15$ ,  $\phi_2 = 0.10$ ,  $r_1 = 0.30$ ,  $r_2 = 0.25$ ,  $r_3 = 1.40$ ,  $r_4 = 1.20$ . The corresponding objective functional values are  $\mathbb{J}(0,0) = 3.9223$  (without controls), and  $\mathbb{J}(u_1^*, u_2^*) = 4.8371$  (with optimal controls). Optimal control pair values are  $u_1 = [0.20, 0.15, 0.13, 0.11, 0.08, 0.06, 0.03, 0.00]$ ,  $u_2 = [0.15, 0.14, 0.12, 0.10, 0.08, 0.06, 0.03, 0.00]$ .

The plots in Figure 9 use the same baseline parameters as those in Figure 6 except for decreasing the augmentation coefficients  $\rho_1$  and  $\rho_2$  from 0.90 and 0.80 to 0.35 and 0.30, respectively. Employing these parameter values, the endangered population levels have reduced as compared to those generated in Figure 6. On the other hand, the plots of the reserve population with optimal controls indicate population levels higher than those generated in Figure 6. Hence, reducing the values of the augmentation coefficients reduces the target population levels and increases the reserve population levels. The values of optimal control pairs are

$$(34) \quad \begin{aligned} u_{1,t} &= [0.20, 0.15, 0.13, 0.11, 0.08, 0.06, 0.03, 0.00], \\ u_{2,t} &= [0.15, 0.14, 0.12, 0.10, 0.08, 0.06, 0.03, 0.00]. \end{aligned}$$

The  $u_{1,t}$  values in (34) show that about 20%, 15%, 13%, 11%, 8%, 6%, and 3% of the reserve  $x_{2,t}$  are translocated for augmentation at time steps  $t = 0, 1, 2, 3, 4, 5$  and 6, respectively. Similarly, the  $u_{2,t}$  values indicate that about 15%, 14%, 12%, 10%, 8%, 6% and 3% of the reserve  $y_{2,t}$  are translocated for augmentation at time steps  $t = 0, 1, 2, 3, 4, 5$  and 6, respectively. No individual of either reserve species is translocated at time step  $t = 7$ . The objective functional values  $\mathbb{J}(0, 0) = 3.9223$  and  $\mathbb{J}(u_1^*, u_2^*) = 4.8371$ , differs by 23%.

## 5. CONCLUSION

In this study, optimal control theory is applied to a model of species augmentation for the competition interaction using discrete difference equations. Four populations that follow the discrete version of the Lotka-Volterra competition model with strong Allee effects are considered. Two of these four populations (i.e., target populations) are initially declining due to small population sizes, and the other two populations (i.e., reserve populations) are kept separately in their habitat and are viable sources for harvesting and translocating individuals for augmentation. The augmentation technique defined in this work aims to maximize the populations at each time step with both linear and quadratic cost functions of the controls. We consider two objective functionals; thus, the first objective functional accounts for both linear and nonlinear increases in the translocation costs of the reserve populations as the proportion translocated at a given time step increases, and the second objective functional accounts for only nonlinear increases in the translocation costs as the proportion translocated at a given time step increases.

Furthermore, the generalization of Pontryagin's Maximum Principle for the optimal control of discrete-time state systems is employed to obtain the necessary conditions. By forming the Hamiltonian functions, we obtain the characterizations of the optimal controls. We employ the discrete version of the forward-backward sweep method in our numerical simulations, utilizing MATLAB R2021a software. In the simulations, long-term and short-term qualitative dynamics of our discrete-time augmentation model are discussed.

The plots of the states and the plots of the corresponding optimal controls in Figures 1 and 6 indicate that the endangered and the reserve populations levels are above the minimum threshold for growth at the end of time steps, and hence, their population will be able to grow after the augmentation effort. In addition, Figure 1 gives the objective functional values  $\mathbf{J}(0,0) = 0.7850$  and  $\mathbf{J}(u_1^*, u_2^*) = 1.3234$ ; showing about 69% higher objective functional value with optimal controls than without optimal controls. Likewise, Figure 6 gives objective functional values  $\mathbb{J}(0,0) = 3.9223$ , and  $\mathbb{J}(u_1^*, u_2^*) = 7.8439$ ; indicating about 100% higher objective functional value with optimal controls than without optimal controls.

Another interesting observation made is the impact of the competition factor. As observed in Figure 4, comparing to the baseline plots in Figure 1, reducing the competition coefficients  $\phi_1$  and  $\phi_2$  from 0.20 and 0.10 to 0.08 and 0.07, respectively, the target populations  $x_{1,t}$  and  $y_{1,t}$  population levels have increased to 0.78 and 0.80, respectively, which are all above the threshold for growth. Further simulations show that increasing competition coefficients reduces the target population levels. For instance, the graphs in Figure 8 were generated using the same baseline parameters as those in Figure 6 except the competition coefficients  $\phi_1 = 0.80$  and  $\phi_2 = 0.75$ , the target population  $x_{1,t}$  shows a very high population level, whilst the target population  $y_{1,t}$  shows a drastic decrease in population level. This illustrates that the competition between species in their ecological habitat can play a crucial role in population extinction.

Again, in Figure 5, decreasing the values of augmentation coefficients,  $\rho_1$  and  $\rho_2$  from 1.2 and 1.0 to 0.35 and 0.30, respectively, the target populations exhibit a decline in population levels, indicating possible extinction of the target species. Similarly, decreasing the augmentation coefficients  $\rho_1$  and  $\rho_2$  from 0.90 and 0.80 to 0.35 and 0.30, respectively, in Figure 9, the endangered population levels have reduced as compared to those generated in Figure 6. In

these same parameter settings, the plots of the reserve population with optimal controls indicate population levels higher than those generated in Figure 6. Therefore, decreasing the values of the augmentation coefficients decreases the target population levels and increases the reserve population levels.

This work provides the foundation of optimal control theory applied to the competition model of discrete-time difference equations. The idea of this work is not limited to competition relationships; it can be extended to other kinds of interaction relationships.

## ACKNOWLEDGEMENTS

The authors are grateful to the Pan African University Institute for Basic Sciences, Technology and Innovation (PAUSTI) for the support.

## CONFLICT OF INTERESTS

The authors declare that there is no conflict of interests.

## REFERENCES

- [1] C. Wolf, W.J. Ripple, Range Contractions of the World's Large Carnivores, *R. Soc. Open Sci.* 4 (2017), 170052. <https://doi.org/10.1098/rsos.170052>.
- [2] W.J. Ripple, J.A. Estes, R.L. Beschta, C.C. Wilmers, E.G. Ritchie, et al., Status and Ecological Effects of the World's Largest Carnivores, *Science* 343 (2014), 1241484. <https://doi.org/10.1126/science.1241484>.
- [3] C. Wolf, W.J. Ripple, Prey Depletion as a Threat to the World's Large Carnivores, *R. Soc. Open Sci.* 3 (2016), 160252. <https://doi.org/10.1098/rsos.160252>.
- [4] A. Hastings, L.J. Gross, *Encyclopedia of Theoretical Ecology*, University of California Press, (2012).
- [5] J.L. ittleman, Extinction, *Britannica*. <https://www.britannica.com/science/extinction-biology>.
- [6] G. Ceballos, P.R. Ehrlich, Mammal Population Losses and the Extinction Crisis, *Science* 296 (2002), 904–907. <https://doi.org/10.1126/science.1069349>.
- [7] J.A. Estes, J. Terborgh, J.S. Brashares, M.E. Power, J. Berger, et al., Trophic Downgrading of Planet Earth, *Science* 333 (2011), 301–306. <https://doi.org/10.1126/science.1205106>.
- [8] M. Dasumani, S. Lenhart, G.K. Onyambu, S.E. Moore, Optimal Control of Species Augmentation in a Competition Model, *Math. Biosci.* 381 (2025), 109394. <https://doi.org/10.1016/j.mbs.2025.109394>.
- [9] Extinct Animals, All That Is Gone, but Not Forgotten. <https://www.extinctanimals.org>.

- [10] , Optimal Control Applied to a Model for Species Augmentation, *Math. Biosci. Eng.* 5 (2008), 669–680. <https://doi.org/10.3934/mbe.2008.5.669>.
- [11] E.N. Bodine, L.J. Gross, S. Lenhart, Order of Events Matter: Comparing Discrete Models for Optimal Control of Species Augmentation, *J. Biol. Dyn.* 6 (2012), 31–49. <https://doi.org/10.1080/17513758.2012.697197>.
- [12] D. Maes, W. Vanreusel, W. Talloen, H.V. Dyck, Functional Conservation Units for the Endangered Alcon Blue Butterfly *Maculinea Alcon* in Belgium (Lepidoptera: Lycaenidae), *Biol. Conserv.* 120 (2004), 229–241. <https://doi.org/10.1016/j.biocon.2004.02.018>.
- [13] P.J. Seddon, A. Moehrenschrager, J. Ewen, Reintroducing Resurrected Species: Selecting DeExtinction Candidates, *Trends Ecol. Evol.* 29 (2014), 140–147. <https://doi.org/10.1016/j.tree.2014.01.007>.
- [14] K. Viggers, D. Lindenmayer, D. Spratt, The Importance of Disease in Reintroduction Programmes, *Wildl. Res.* 20 (1993), 687–698. <https://doi.org/10.1071/wr9930687>.
- [15] S.M. Cheyne, Wildlife Reintroduction: Considerations of Habitat Quality at the Release Site, *BMC Ecol.* 6 (2006), 5. <https://doi.org/10.1186/1472-6785-6-5>.
- [16] M. Plein, M. Bode, M.L. Moir, P.A. Vesk, Translocation Strategies for Multiple Species Depend on Interspecific Interaction Type, *Ecol. Appl.* 26 (2016), 1186–1197. <https://doi.org/10.1890/15-0409>.
- [17] K.A. Romain-Bondi, R.B. Wielgus, L. Waits, W.F. Kasworm, M. Austin, et al., Density and Population Size Estimates for North Cascade Grizzly Bears Using DNA Hair-Sampling Techniques, *Biol. Conserv.* 117 (2004), 417–428. <https://doi.org/10.1016/j.biocon.2003.07.005>.
- [18] P. Bouley, A. Paulo, M. Angela, C. Du Plessis, D.G. Marneweck, The Successful Reintroduction of African Wild Dogs (*Lycaon Pictus*) to Gorongosa National Park, Mozambique, *PLOS ONE* 16 (2021), e0249860. <https://doi.org/10.1371/journal.pone.0249860>.
- [19] M. Funabashi, Augmentation of Plant Genetic Diversity in Synecoculture: Theory and Practice in Temperate and Tropical Zones, *Sustain. Dev. Biodivers.* 22 (2019), 3–46. [https://doi.org/10.1007/978-3-319-96454-6\\_1](https://doi.org/10.1007/978-3-319-96454-6_1).
- [20] A. Povilitis, Characteristics and Conservation of a Fragmented Population of Huemul *Hippocamelus Bisulcus* in Central Chile, *Biol. Conserv.* 86 (1998), 97–104. [https://doi.org/10.1016/s0006-3207\(97\)00161-4](https://doi.org/10.1016/s0006-3207(97)00161-4).
- [21] J. Hearne, J. Swart, Optimal Translocation Strategies for Saving the Black Rhino, *Ecol. Model.* 59 (1991), 279–292. [https://doi.org/10.1016/0304-3800\(91\)90182-z](https://doi.org/10.1016/0304-3800(91)90182-z).
- [22] M. Pfab, E. Witkowski, A Simple Population Viability Analysis of the Critically Endangered *Euphorbia Clivicola* R.A. Dyer Under Four Management Scenarios, *Biol. Conserv.* 96 (2000), 263–270. [https://doi.org/10.1016/s0006-3207\(00\)00088-4](https://doi.org/10.1016/s0006-3207(00)00088-4).
- [23] P.W. Hedrick, Gene Flow and Genetic Restoration: The Florida Panther as a Case Study, *Conserv. Biol.* 9 (1995), 996–1007. <https://doi.org/10.1046/j.1523-1739.1995.9050996.x>.



- [24] P.J. Manlick, J.E. Woodford, J.H. Gilbert, D. Eklund, J.N. Pauli, Augmentation Provides Nominal Genetic and Demographic Rescue for an Endangered Carnivore, *Conserv. Lett.* 10 (2016), 178–185. <https://doi.org/10.1111/conl.12257>.
- [25] E. Bodine, M. Martinez, Optimal Genetic Augmentation Strategies for a Threatened Species Using a Continent-Island Model, *Lett. Biomath.* 1 (2014), 23–39. <https://doi.org/10.30707/lib1.1bodine>.
- [26] C.M. Taylor, A. Hastings, Allee Effects in Biological Invasions, *Ecol. Lett.* 8 (2005), 895–908. <https://doi.org/10.1111/j.1461-0248.2005.00787.x>.
- [27] F. Courchamp, L. Berec, J. Gascoigne, *Allee Effects in Ecology and Conservation*, Oxford University Press, 2008. <https://doi.org/10.1093/acprof:oso/9780198570301.001.0001>.
- [28] W.C. Allee, *The Social Life of Animals*, W.W. Norton & Company, 1938.
- [29] P.A. Stephens, W.J. Sutherland, R.P. Freckleton, What Is the Allee Effect?, *Oikos* 87 (1999), 185–190. <https://doi.org/10.2307/3547011>.
- [30] S.R. Jang, Competitive Exclusion and Coexistence in a Leslie–Gower Competition Model with Allee Effects, *Appl. Anal.* 92 (2013), 1527–1540. <https://doi.org/10.1080/00036811.2012.692365>.
- [31] D.S. BOUKAL, L. BEREK, Single-Species Models of the Allee Effect: Extinction Boundaries, Sex Ratios and Mate Encounters, *J. Theor. Biol.* 218 (2002), 375–394. <https://doi.org/10.1006/jtbi.2002.3084>.
- [32] F. Courchamp, T. Clutton-Brock, B. Grenfell, Inverse Density Dependence and the Allee Effect, *Trends Ecol. Evol.* 14 (1999), 405–410. [https://doi.org/10.1016/s0169-5347\(99\)01683-3](https://doi.org/10.1016/s0169-5347(99)01683-3).
- [33] G.A. Maciel, F. Lutscher, Allee Effects and Population Spread in Patchy Landscapes, *J. Biol. Dyn.* 9 (2015), 109–123. <https://doi.org/10.1080/17513758.2015.1027309>.
- [34] J. Musgrave, A. Girard, F. Lutscher, Population Spread in Patchy Landscapes Under a Strong Allee Effect, *Theor. Ecol.* 8 (2015), 313–326. <https://doi.org/10.1007/s12080-015-0252-1>.
- [35] S. Grey, S. Lenhart, F.M. Hilker, D. Franco, Optimal Control of Harvest Timing in Discrete Population Models, *Nat. Resour. Model.* 34 (2021), e12321. <https://doi.org/10.1111/nrm.12321>.
- [36] A. El Bhih, Y. Benfatah, S. Ben Rhila, M. Rachik, A. El Alami Laaroussi, A Spatiotemporal Prey-Predator Discrete Model and Optimal Controls for Environmental Sustainability in the Multifishing Areas of Morocco, *Discret. Dyn. Nat. Soc.* 2020 (2020), 2780651. <https://doi.org/10.1155/2020/2780651>.
- [37] A.J. Whittle, S. Lenhart, L.J. Gross, Optimal Control for Management of an Invasive Plant Species, *Math. Biosci. Eng.* 4 (2007), 101–112. <https://doi.org/10.3934/mbe.2007.4.101>.
- [38] J.D. Murray, *Mathematical Biology I. An Introduction*, Springer New York, 2002. <https://doi.org/10.1007/b98868>.
- [39] L.B. Slobodkin, *Growth and Regulation of Animal Populations*, Dover Publications, (1980).
- [40] R. Levins, D. Culver, Regional Coexistence of Species and Competition Between Rare Species, *Proc. Natl. Acad. Sci.* 68 (1971), 1246–1248. <https://doi.org/10.1073/pnas.68.6.1246>.

- [41] H.S. Horn, R.H. MacArthur, Competition among Fugitive Species in a Harlequin Environment, *Ecology* 53 (1972), 749–752. <https://doi.org/10.2307/1934797>.
- [42] A. Hastings, Disturbance, Coexistence, History, and Competition for Space, *Theor. Popul. Biol.* 18 (1980), 363–373. [https://doi.org/10.1016/0040-5809\(80\)90059-3](https://doi.org/10.1016/0040-5809(80)90059-3).
- [43] S. Nee, R.M. May, Dynamics of Metapopulations: Habitat Destruction and Competitive Coexistence, *J. Anim. Ecol.* 61 (1992), 37–40. <https://doi.org/10.2307/5506>.
- [44] D. Tilman, Competition and Biodiversity in Spatially Structured Habitats, *Ecology* 75 (1994), 2–16. <https://doi.org/10.2307/1939377>.
- [45] P. Liu, S.N. Elaydi, Discrete Competitive and Cooperative Models of Lotka–Volterra Type, *J. Comput. Anal. Appl.* 3 (2001), 53–73. <https://doi.org/10.1023/a:1011539901001>.
- [46] M. Kot, *Elements of Mathematical Ecology*, Cambridge University Press, 2001. <https://doi.org/10.1017/cbo9780511608520>.
- [47] S. Hsu, S. Hubbell, Two Predators Competing for Two Prey Species: An Analysis of MacArthur’s Model, *Math. Biosci.* 47 (1979), 143–171. [https://doi.org/10.1016/0025-5564\(79\)90035-x](https://doi.org/10.1016/0025-5564(79)90035-x).
- [48] L.S. Pontryagin, V.G. Boltyanskii, R.V. Gamkrelidze, E.F. Mischenko, *The Mathematical Theory of Optimal Processes*, Wiley, 1962.
- [49] S. Lenhart, J.T. Workman, *Optimal Control Applied to Biological Models*, Chapman and Hall/CRC, 2007. <https://doi.org/10.1201/9781420011418>.